Acoustics Measurement Buoy

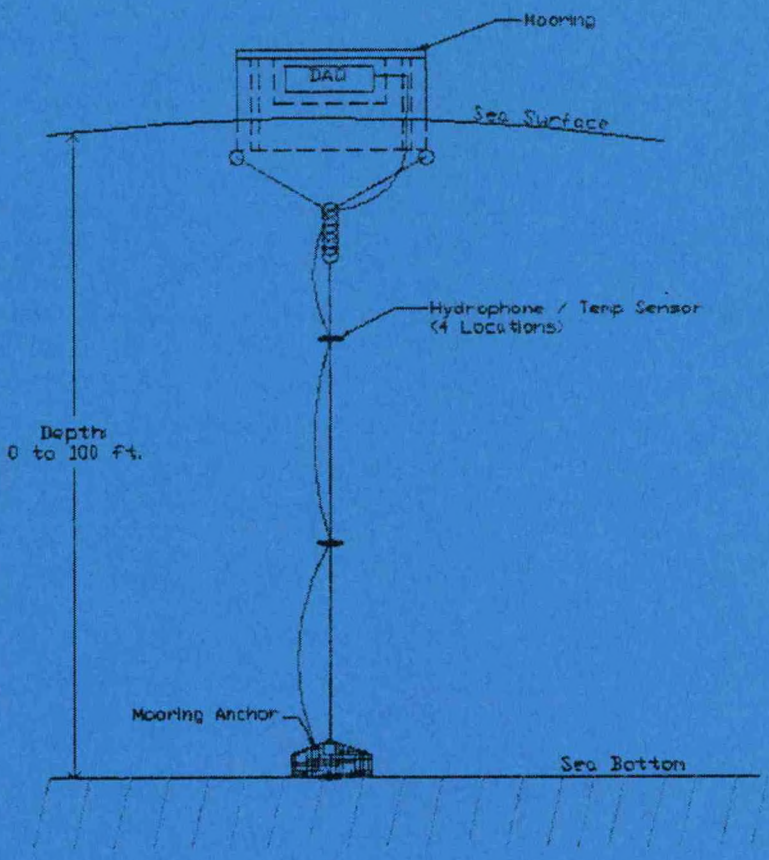

Team Members
Laurel Gaudet
Kevin Jerram
Ashley Risso

Team Advisor
Dr. Kenneth C. Baldwin

TECH797 2005 – 2006
Undergraduate Ocean Research Projects
University of New Hampshire

Submitted April 21, 2006

Sea Grant
New Hampshire


NOAA
NATIONAL OCEANIC AND ATMOSPHERIC ADMINISTRATION
U.S. DEPARTMENT OF COMMERCE

Acknowledgements

This work is the result of research sponsored, in part, by the National Sea Grant College Program, NOAA, Department of Commerce, under grant #NA16RG1035 through the New Hampshire Sea Grant College Program

The Acoustics Measurement Buoy team would like to thank the many individuals who have generously given countless hours of their time, shared technical and practical advice, and supported all phases of design, construction, and testing of our prototype.

We would like to thank our advisor and mentor Ken Baldwin for his genuine interest in all stages of our project and for supporting future work based on our prototype.

Many individuals in the Ocean Engineering department assisted our team by answering questions, helping to develop realistic design goals, providing time-saving construction advice, and lending tools, equipment, and supplies. Paul LaVoie, Jim Irish, Andy McLeod, Glen McGillicuddy, Stanley Boduch, and Judson DeCew were each instrumental to many important steps along the development of this project. We would like to thank members of the UNH Hovercats team for their tremendous help and donation of materials during surface buoy construction. Our team owes a debt of gratitude to Dave Moceri for his enthusiasm, encouragement, and commitment throughout this project, and wishes him the best during his graduate work.

Our team and many others would like to thank Jon Scott and M. R. Swift for coordinating the TECH797 Ocean Undergraduate Research Projects class to offer exciting alternatives to conventional Mechanical Engineering department projects. Project funding and expedited processing of budgetary items by Jon Scott is greatly appreciated.

Table of Contents

List of Figures

List of Tables

List of Equations

Abstract

This report discusses the progress of the Acoustics Measurement Buoy project as part of the University of New Hampshire's Ocean Projects TECH 797 class, Undergraduate Ocean Research Projects. Fish shock and mortality have been linked with sound pressure levels in excess of 190 dB (re 1 μPa) associated with pile driving into marine sediments in estuaries and surrounding areas. The Acoustics Measurement Buoy was designed to measure and record sound pressure levels at multiple depths over multiple deployments to aid in modeling sound attenuation around estuarine construction sites and allow in-field evaluation of sound attenuation techniques developed for pile driving activities.

A taut mooring line supports multiple hydrophones at different depths to measure sound pressure level (SPL) and temperature loggers to record temperature at the depths of sound pressure measurements. Hydrophone signals are transmitted to a central data acquisition system housed in a surface buoy. The system is intended to be deployed at various distances from the sound source in order to measure changes in SPL with distance. Three ranges of sound pressure level are of specific interest during pile driving activities: where SPL > 220 dB, 180 dB < SPL < 220 dB, and SPL < 180dB. The Acoustics Measurement Buoy may be used for on-site evaluation of sound attenuation techniques used during pile driving activities.

Background

Pile driving associated with construction in estuarine regions, such as reconstruction of the San Francisco-Oakland Bay Bridge, is a significant source of submarine acoustic disturbances. This project is intended to aid in development of better understanding of waterborne noise propagation in marine construction zones. Combined with biological studies done on fisheries, research into noise propagation around marine construction sites will allow further development and evaluation of techniques for sound pressure level reduction in sensitive spawning regions and surrounding fisheries. Pictures of the San Francisco-Oakland Bay Bridge and a pile being driven are presented below in Figure 1.

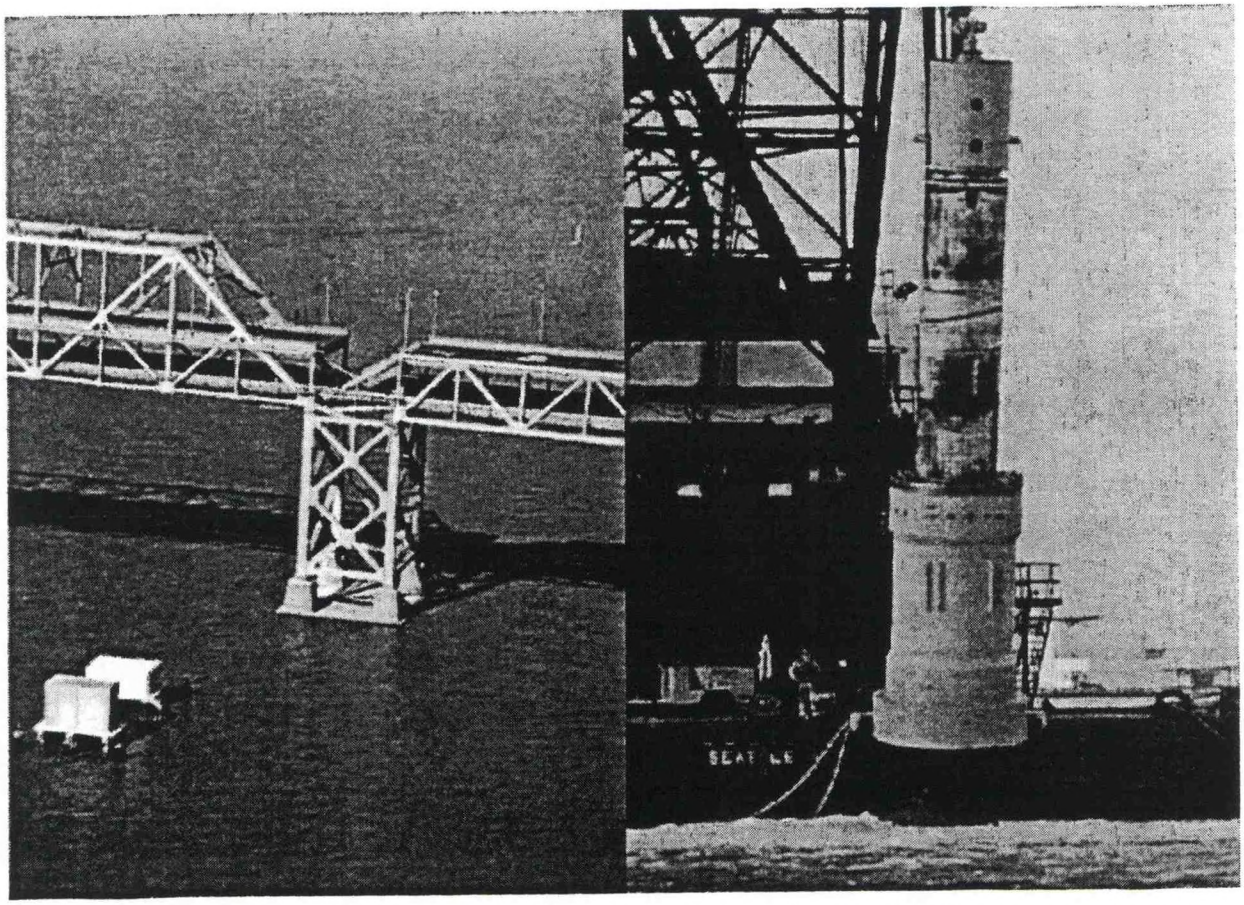

Figure 1: (L-R) San Francisco-Oakland Bridge Construction and pile driving operations

Objective

The objective of this project is to develop a portable, robust, and inexpensive system for measurement of waterborne construction noise associated with construction in coastal and estuarine regions. A sketch of the conceptual design is presented below in Figure 2.

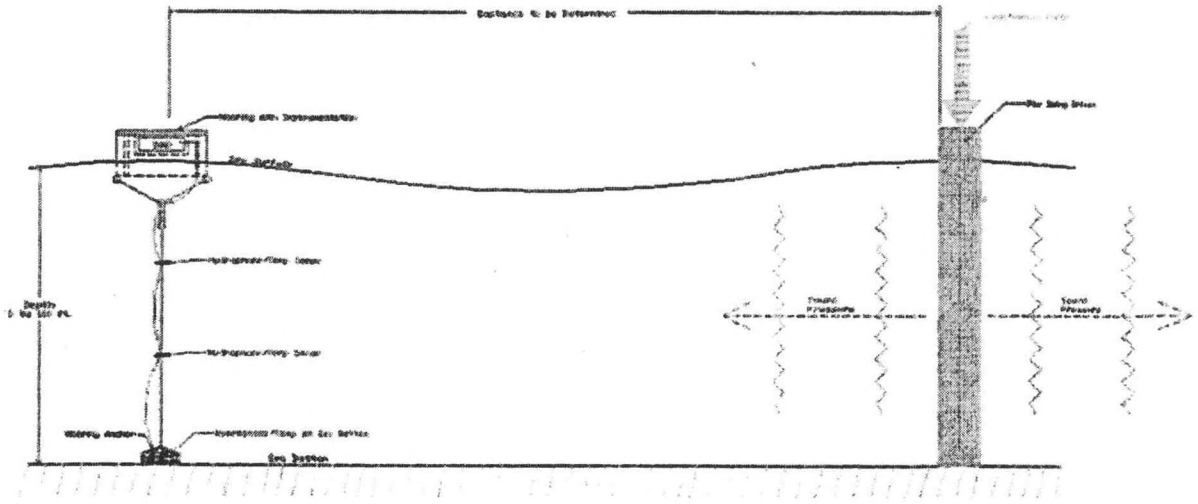

Figure 2: Conceptual outline of sound source and measurement system

Introduction

A mooring and data acquisition system was designed by TECH 797 students to provide a portable and robust tool for measurement of underwater sound profiles at multiple locations near marine construction sites. Most construction-related waterborne noise occurs at frequencies less than 4000 Hz. As such, the primary observation elements are three hydrophones constructed with a target operating frequency range of 10-10,000 Hz. Waterproof data cable runs from each hydrophone along the length of the mooring line and into the data acquisition system housed in the surface float. The data processing unit was designed and built around a VIA EPIA motherboard running Microsoft Windows XP and National Instruments LabVIEW software for on-board noise filtration and analog-to-digital conversion, with sample frequencies of up to 100 kS/s. A 100 GB hard drive and wireless networking card provide ample data storage and means of remote control of the measurement system. Self-contained temperature recorders with programmable sampling frequency and internal data storage are mounted with each of the three hydrophones to help measure effects of temperature on sound propagation.

Theory

Noise in the water column is caused by many sources. Significant sources of underwater noise are construction projects in and around waterways. Pile driving with hydraulic hammers causes acoustic waves with sound pressure levels (SPL) of up to 260 dB re 1μPa. It has been proven that these pressure waves affect animal life and can burst the swim bladders of some marine creatures. The most extensive studies of acoustic effects on marine life have been done on fish. Results of these studies are presented in the 2001 paper by Hastings in which he indicated that "little or no physical damage to aquatic animals would be expected for peaks and pressure below 190 dB re 1μPa." Damage begins to occur over 190 dB re 1μPa. Most pile driving activities produce sound source levels between 180 and 260 dB re 1μPa.

Acoustic Theory

The vibration that occurs after a pile has been hit creates compression waves which move from the pile into the water column and medium into which the pile is being driven. As these waves propagate away from the pile, their energy is spread across a cylindrical or spherical wave front of increasing radius. The speed of these waves can be calculated using

Sound Speed $c = \sqrt{\frac{\kappa + 4/3\mu}{\rho}}$

μ= rigidity
κ= bulk modulus (1/compressibility)
ρ= density

Equation 1: Speed of sound

The speed of sound in water is controlled by temperature, pressure and salinity, in this order of importance. The rate of change of velocity is generally estimated to change by approximately 3m/s/°C with temperature, 0.017m/s/m with pressure (depth), and 1.2m/s/ppt with salinity. The actual speed of sound in water can be calculated using the MacKenzie Equation,

$$C = 1448.96 + 4.591T - 5.304*10^{-2}T^2 + 2.374*10^{-4}T^3 + 1.340(S-35) + 1.630*10^{-2}D + 1.675*10^{-7}D^2 - 1.025*10^{-2}T(S-35) - 7.139*10^{-13}TD^3$$

Equation 2: Speed of sound in water

Sound pressure level is measured by the hydrophone. Using the hydrophone sensitivity, amplifier gain, and the RMS value of the hydrophone output voltage, the sound pressure level (SPL) can be determined by

$$SPL=|Mx|-G+20\log V,$$

Equation 3: Sound pressure level

where Mx is the voltage sensitivity of the hydrophone [dB re 1 V/μPa], G is the gain [dB], and V is the hydrophone output voltage [V].

Intensity at the wave front decreases as the wave is subject to transmission loss during propagation through the transmission medium. Transmission loss (TL) occurs due to conservation of energy over an ever-increasing geometrical wave front and absorption of the pressure wave due to viscous losses on the molecular level. Geometric transmission loss is calculated by assuming either a cylindrical or spherical spreading model for the wave front. In general,

$$TL=10\log(I(1m)/I(r)),$$

Equation 4: Transmission loss

where I(1m) is the intensity at one meter from the source and I(r) is the intensity at radius r, measured in meters.

Solving for wave front surface area as a function of radius and substituting into Equation 4, transmission loss is calculated in the cylindrical spreading model by

$$TL_{geo}=10\log(r),$$

Equation 5: Geometrical transmission loss in cylindrical spreading model

and in the spherical spreading model by

$$TL_{geo}=20\log(r),$$

Equation 6: Geometrical transmission loss in spherical spreading model

where TL_{geo} is measured in dB re 1μPa and r is the radius in meters from the source. Total transmission loss is the sum of geometric losses plus absorption losses, such that

$$TL=TL_{geo}+TL_{abs}.$$

Equation 7: Total transmission loss

Transmission loss due to absorption is a function of frequency and is usually extremely small compared to geometric transmission loss. Acoustic waves with frequencies in the operating range of the measurement system (10-10,000 Hz) have extremely low absorption losses over reasonable distance scales. For this reason, absorption losses usually have units of dB re 1μPa per kilometer. Because the distances from the source to the deployed system are intended to be less than one kilometer, transmission losses due to absorption are neglected.

Design Approach – Equipment Specifications

Acoustics and Electronics

Hydrophones

Omnidirectional hydrophones are to be employed for measurement of local sound pressure level (SPL) values at a radius from a pile driving event. To better understand sound propagation through different layers of the estuarine environment, three hydrophones are to be mounted along the mooring line at different depths. Due to the nature of vibration anticipated for large-diameter pile driving, the desired hydrophone frequency range is limited between 10 – 4000 Hz, which is a relatively low range by industry standards. Low-frequency hydrophones are desired with internal preamplifiers to guarantee signal strength over the length of cable between the measurement device and data acquisition system. Low power consumption is desired for extended battery life and reduced thermal effects. Light weight and relatively compact, sleek shape are desired for ease of deployment and minimal hydrodynamic drag in currents.

Geophone

A geophone used to measure ground-borne acoustic propagation is to be mounted in close proximity to the mooring ballast. Desired geophone operating parameters coincide with those outlined in the hydrophone specification; a frequency range of 10 – 4000 Hz, internal preamplification, and low power consumption are of primary importance. Ease of geophone mounting is also of particular concern, as a special mounting mechanism must be developed to use the ballast to aid in planting the geophone without crushing the device.

Temperature Loggers

A method of temperature measurement is needed at the depth of sound pressure measurement in the water column along the mooring line. Depth measurement for each instrument package was considered but eliminated because, using a taut mooring system, the height of the sensors above the seafloor is considered constant. Waterproof construction, programmable sample rate (10 S/s), and low power consumption are the primary considerations in selecting temperature loggers.

Data Acquisition - General

Four channels of hydrophone and geophone data are to be filtered, stored, and retrieved using a data acquisition system consisting of a trigger, low-pass filter, data logging hardware and software, and either a portable flash-memory drive or wireless data retrieval mechanism. If necessary, an analog-to-digital converter (ADC) may be employed after filtration and before data logging. All data acquisition hardware is to be contained in a sealed pressure vessel housed within the main buoy. A conceptual diagram of the data acquisition layout is presented below in Figure 3.

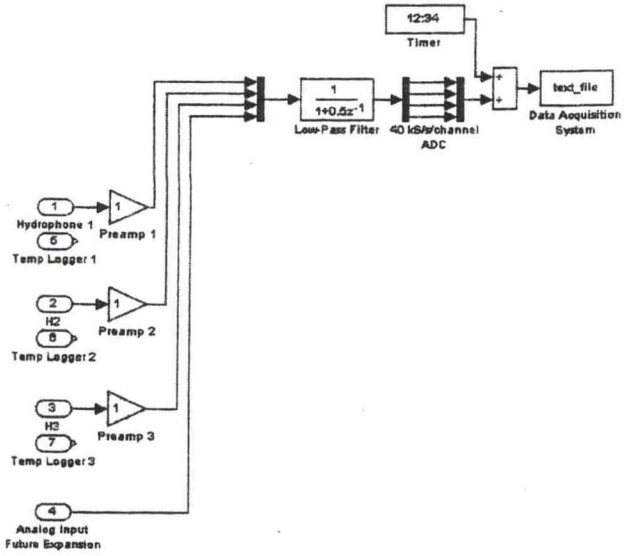

Figure 3: Conceptual flow diagram for data acquistions system

Low-Pass Filter

To better mitigate high-frequency noise in the data acquisition system and ensure measurement of only low-frequency construction-related acoustic data, a simple low-pass filter with cutoff frequency of 4 kHz is desired for filtration of each channel prior to data logger input. Reliability, low cost, and low power consumption are of primary importance. A single device with four-channel analog inputs and outputs would be preferred over four individual filters.

Analog-to-Digital Converter

The data logger must sample four analog inputs at a minimum rate of 40 kS/s per channel, or 10 times the maximum expected frequency per channel according to the Nyquist criterion. Sampling four channels at this rate yields an aggregate sampling frequency of 160 kS/s. For greatest resolution of measurements, 16-bit sampling resolution is desired. Required data logger memory depends on the desired duration of measurements. For one hour of measurement using three hydrophones and one geophone with 16-bit resolution and an aggregate sampling frequency of 160 kS/s, approximately 1.2 GB of internal memory is required. As such, a four-channel data logger is desired with an aggregate sampling frequency of at least 200 kS/s, 16-bit resolution, and internal memory of 2 GB. Considering the cost of lost data and boat time, data logger reliability is of great importance. Minimal size and power consumption are desired for increased packaging options and reduced thermal effects in the main data acquisition system housing.

Data Retrieval

Ease and speed of data retrieval for analysis is critical for utility of the entire measurement system. Portable flash-memory devices, known as "flashdrives," are available in many sizes (including sizes greater than 1 GB) and allow plug-and-play versatility for data storage options.

Portable USB-style flashdrives are relatively inexpensive, robust, and accepted by nearly all modern laptop computers. Use of multiple USB-style flashdrives would allow simultaneous off-shore measurement and on-deck analysis of previous data between measurement periods. While the anticipated low cost of flashdrive storage makes this data retrieval method attractive, the physical exchange of USB flashdrives in the main data acquisition compartment presents safety hazards to users of the monitoring system during deployment. To largely eliminate personnel risk associated with data retrieval after deployment, a wireless data transfer method may be considered. Such a system would require a dedicated internal data storage device to be coupled with certain wireless networking hardware to establish a local network between the measurement computer and a remote computer. A backup method for hardwired data transfer must be built-in to the data acquisition system.

Wireless Control

Remote activation of the measurement system is desired for ease of measurement control after deployment. If remote start-up is not possible, then wireless control of the start and stop times for measurement is desired after start-up of the data acquisition system. A hardwire connection between a remote computer and the data acquisition system should be available if wireless connection quality is inadequate or unavailable due to environmental interference.

Battery

A marine battery must be sized to accommodate all hydrophone, geophone, and data acquisition system voltage requirements for the duration of several hours of measurement. To prevent disturbance of voltage-sensitive devices, an external power switch and low-power alarm device is desired to ensure proper shutdown of the data acquisition system.

Mooring & Buoy Specifications

A mooring system that has the capability to hold the buoy in place in the water column needed to be designed. In order to mitigate hydrophone displacement due to varying current and tidal stages, a taut-line mooring design was considered. With variable tides and sea states, a compliant member would need to be included in the main mooring line. A ballast calculation was needed in order to ensure that the buoy would not be pulled off the sea floor. To attach the mooring line to the buoy, a lightweight system which did not interfere with the submerged canister was desired.

To obtain a mooring design adequate for these parameters average environmental conditions of potential test sites were researched. These criteria were then fed into a marine finite element analysis program (AquaFE), which is discussed in the preliminary analyses section.

Average Estuarine Conditions for Sample Test Sites

In order to make an accurate model of a location the buoy would be deployed in, data were obtained from three sites. Each of these sites had an ongoing bridge construction project and was seen as a location where fauna could be affected by pile driving. Average weather conditions and river characteristics were collected and entered into a simulation model of the buoy.

The sites included the Manhattan River Bridge, bridge construction over the East River in Manhattan New York, The Penobscot Bay Bridge, crossing the Penobscot River in Bucksport, Maine, and the Susquehanna River Bridge project in Harrisburg, Pennsylvania. Data were obtained from the United States Geologic Survey (USGS) and the National Oceanographic and Atmospheric Administration (NOAA).

Information gathered for each site included the average water temperature at that location, the average wind speed in that area, the depth of the river, any tidal or wave influence, and the average current. Table 2 displays the results of the data collection.

Table 1: Data for each bridge site

Sample Weather Conditions at Bridge Sites			
	ME	PA	NY
Wind (mph)	6	4.55	5
Depth (ft)		6	5
Velocity (ft/s)		3.12	1.1
Current flow (ft3/s)	15000	38600	100
	Great Bay	Piscataqua	
Tidal flux (m)	2	3	
Wind (mph)		6	
Current (knts)	6	8	

Buoy

In order to establish a minimum buoyancy requirement for the surface buoy, the weights of all elements of the system were calculated or estimated. It was determined that a buoy with approximately 200 lbs of buoyancy would need to be constructed. The floatation material would need the ability to be formed or cut into a cylinder with an inner diameter region removed for data acquisition system housing. Because it would be deployed in salt water, the outer cover would need to be waterproof and corrosion-resistant.

Design Approach – Selected Equipment

Acoustics and Electronics

Hydrophones

Preassembled and calibrated omnidirectional hydrophones with low-frequency operating ranges were researched and determined to cost approximately $1000 each from several manufacturers.

With a nominal budget of $2500 and a desired quantity of three hydrophones, methods of cost reduction for noise measurement were explored. Expired US Navy sonobuoys, used for active and passive tracking of submarines, were researched for sourcing of suitable hydrophone elements and associated electronics. Several model AN/SSQ-53A DIFAR sonobuoys were donated by Woods Hole Oceanographic Institute and disassembled to determine feasibility of hydrophone sourcing from this model. A picture of the hydrophone and associated filters and electronics is presented below in Figure 4. It was determined that the AN/SSQ-53A hydrophone did not have the omnidirectional frequency response characteristics desired for our application. Sonobuoy model AN/SSQ-57B were researched and determined to employ a desirable low-frequency omnidirectional hydrophone, but were unavailable for disassembly. Sparton Electronics, manufacturer of the hydrophone elements used in the AN/SSQ-57B, offered a quote of $1000 per hydrophone element.

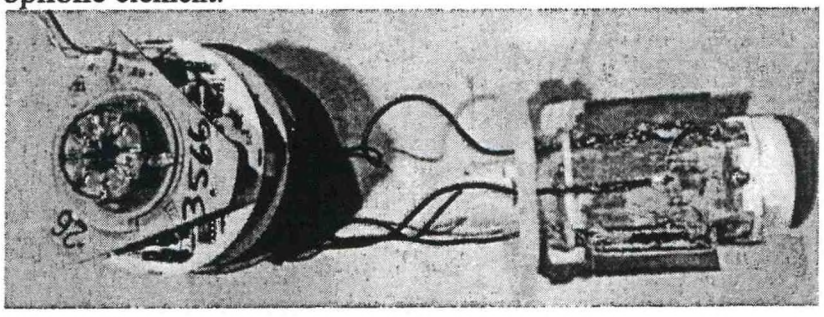

Figure 4: Hydrophone element and associated electronics removed from AN/SSQ-53A sonobuoy manufactured by Sparton Electronics.

Low-cost piezoelectric hydrophone elements and preamplifiers manufactured by Teledyne Benthos were researched, with quoted prices of $50 per element and $335 per preamplifier. Three sets of elements and preamplifiers were purchased for construction of three simple, low-frequency, omnidirectional hydrophones. Manufacturer specifications for the hydrophone elements and preamplifiers are presented in Appendix E.

Hydrophone construction required connection of the hydrophone element and preamplifier in a non-corrosive container for protection of the electronics from saline water. In this configuration, the hydrophone assembly required a long, slender cylindrical housing with cable exiting from one end for connection to the data acquisition system. Reinforced braided vinyl tubing with an inner diameter of ¾" was selected for housing material based on its low cost, abrasion resistance, and ease of modification for

hydrophone assembly. Housing ends were fabricated out of ¾"-diameter, 1 ½"-long barbed PVC plugs filled with marine epoxy putty, inserted into each end of the vinyl housing and secured with stainless steel pipe clamps. A non-electrolytic fluid was required to fill the container for transmission of the acoustic signal from the container wall to the element. Mineral oil was selected as a suitable filler fluid for hydrophone construction based on its nearly-incompressible and environmentally-benign properties. To ensure complete absence of air bubbles in the hydrophone assembly, brass bleed tubes with stainless steel screws, rubber seals, and brass washers were incorporated into each hydrophone end to allow bleeding with mineral oil. A schematic of the hydrophone assembly is shown below in Figure 5.

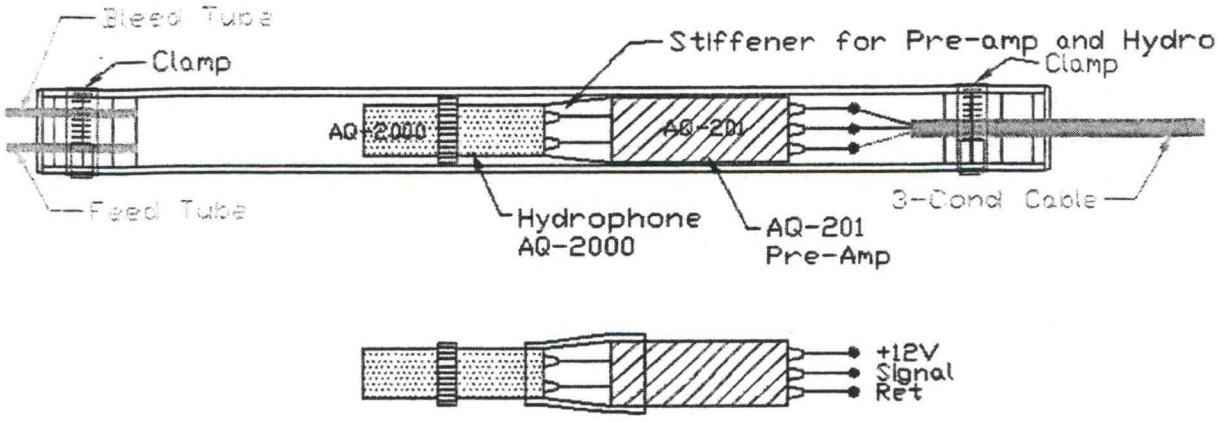

Figure 5: Schematic of hydrophone assembly showing piezoelectric element and preamplifier bathed in mineral oil and housed in vinyl tubing with three-conductor PVC-insulated shielded cable.

The preamplifier requires independent conductors for power supply from a 12VDC voltage source, for electrical grounding, and for signal transmission to the data acquisition system. Standard PVC-insulated cable with three 22-gauge shielded conductors was selected for hydrophone cable.

Equal spacing between the sea floor, hydrophones, and sea surface were desired, with a maximum expected estuary depth of 100 feet; as such, nominal hydrophone cable lengths of 75 feet, 50 feet, and 25 feet were selected. Lengths of ten feet for changes in sea surface height and ten feet for cable routing around the mooring hardware and buoy were added to each hydrophone cable, bringing the total cable lengths to 95 feet, 70 feet, and 45 feet for hydrophones H1, H2, and H3, respectively.

Geophone

Due to budgetary constraints, a geophone was not researched heavily or purchased. However, the data acquisition system can accommodate a fourth analog input, which may be used in the future for a geophone.

Temperature Loggers

The Onset Corporation designed and produced the set of four Pendant loggers. Each logger has 10-bit resolution and 64K of memory. They are waterproof and contain batteries that have a typical run life of one year. The temperature loggers will be

deployed along side the hydrophones at set depths along the mooring cable. In order to retrieve the data the mooring will have to be pulled up and each logger downloaded using the included software.

Data Acquisition - General

All data acquisition hardware for digital sampling and storage of analog hydrophone inputs was selected using the aforementioned criteria and with consideration of the extreme and/or rough environmental conditions the system may be deployed under. The complete data acquisition system consists of a central processing unit motherboard (CPU), analog-to-digital converter (ADC), power supply (PS), hard drive (HD), memory (RAM), wireless network card, and battery. Microsoft Windows XP was selected as the operating system for ease of compatibility with future software applications. National Instruments (NI) LabVIEW software is used with a NI ADC to sample, process, and store hydrophone signals. A simple LabVIEW program for low-pass signal filtration and data storage was written and loaded as an executable onto the data acquisition system. This executable can be programmed to run automatically after start-up of the CPU. All hardware was assembled in a compact configuration, using a custom-built frame of aluminum L-section bar stock and stainless and nylon hardware. Figure 6 and Figure 7, below, present two views of the main data acquisition system and identify major components of the assembly.

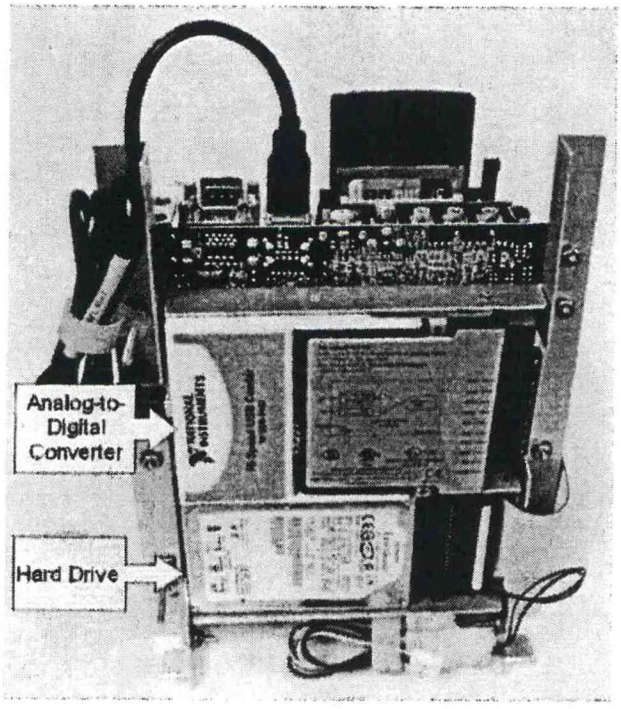

Figure 6: View of ADC, hard drive, and underside of motherboard in data acquisition assembly

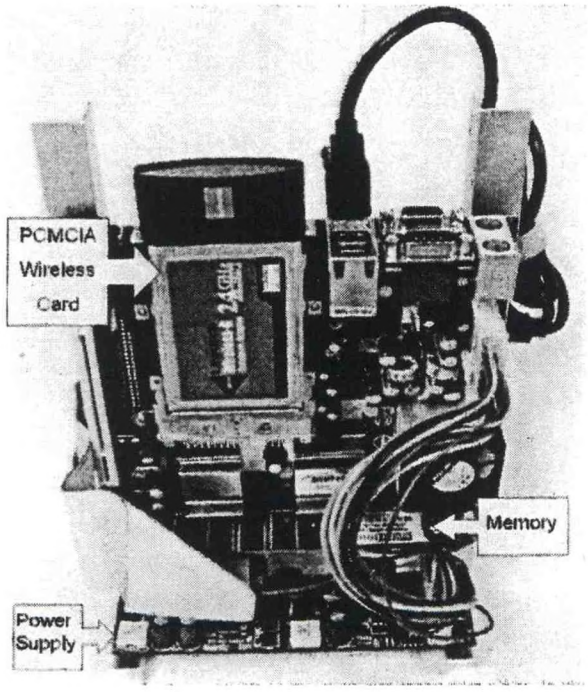

Figure 7: View of wireless networking hardware, power supply, memory, and top side of motherboard.

Low-Pass Filter

National Instruments LabVIEW offers programmable input signal filtration which is used in lieu of an external low-pass filter. A low-pass filter with a cutoff frequency of 4 [kHz] is incorporated into the simple data acquisition program.

Analog-to-Digital Converter

National Instruments model USB-9215A was selected to digitally sample analog hydrophone input. This model is capable of sampling up to four analog channels with sample rates of 100 kS/s/channel, and was chosen for its ease of USB2.0 connectivity with the motherboard, compact size, low power consumption, and affordability. NI LabVIEW drivers are required to run the ADC. Manufacturer specifications for the NI USB-9215A are included in Appendix F. A schematic of hydrophone and ADC wiring is presented below in Figure 8.

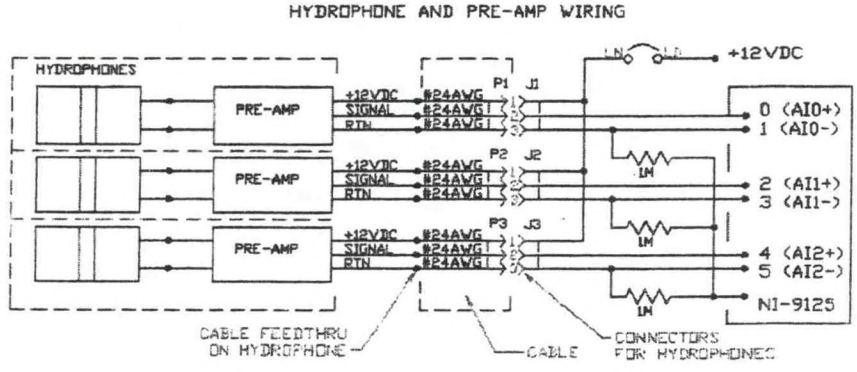

Figure 8: Schematic of hydrophone and ADC electrical configuration

CPU Mainboard

Originally designed for use with in-car entertainment systems, the VIA EPIA MII10000 mainboard has a 1 GHz processor and multiple ports for a monitor, keyboard, USB-compatible accessories, and a PCMCIA wireless networking card. This mainboard was selected for its affordability and versatility to serve as the heart of the data acquisition system, allowing execution of a NI LabVIEW application for signal sampling, enabling data storage on the hard drive, and supporting communication between the system and a remote master computer. The extensive mainboard user's manual is not included in the Appendix, but is available for download at http://www.via.com.tw/download/mainboards/3/4/um_epia-mii_v150.pdf.

Power Supply

Total power consumption for the CPU, ADC, HD, RAM, and wireless adapter is estimated at 30W and requires a 12VDC voltage source. The model M1-ATX power supply, intended for in-car entertainment systems, was selected for its robust design, relatively high 90W power capacity, 12VDC compatibility, and soft-shutdown feature. The soft-shutdown feature helps to ensure a safe shutdown of the mainboard if extreme sea roughness or mishandling compromise any connections between the battery and data acquisition system. Manufacturer specifications for the M1-ATX power supply are included in Appendix F.

Hard Drive

Reliability and ample capacity were the primary concerns when selecting a hard drive. Sampling four channels at a rate of 40 [kS/s/channel] with 16-bit resolution requires approximately 1.2 GB of storage per hour of measurement; in a worst-case scenario, it is desirable to deploy the data acquisition system on multiple occasions for several hours each without overwriting any previous data. To ensure ample capacity and reliability, a 100GB Hitachi Travelstar 5K100 laptop hard drive was selected. This hard drive is well-received for its compact size, quiet operation, low heat dissipation, low power consumption, and generally robust design. A desktop-to-laptop hard drive converter cable was required for installation. Manufacturer specifications for the Hitachi Travelstar 5K100 hard drive are included in Appendix F.

Memory

Economy-quality Corsair 512MB 184-pin DDR SDRAM memory was selected for its affordability and reliability.

Wireless Network Card

A Linksys WPC54G wireless networking card was chosen for its PCMCIA compatibility with the mainboard and 802.11b/g wireless connection capability. Coupled with a Linksys WUSB54G wireless adapter on the master computer, data transfer rates up to 54 Mbps are possible with the 802.11g connection. If the 802.11g connection fails, the wireless adapters revert to an 802.11b connection with data transfer rates of 11 Mbps. Wireless networking should be possible with a clear line-of-sight up to several hundred feet between the data acquisition system and master computer. Manufacturer

specifications for the Linksys WPC54G and WUSB54G wireless networking hardware are included in Appendix F.

Wireless Control

Remote control of the data acquisition system is accomplished using the "Remote Desktop Connection" option available on any computer equipped with a wireless card and Microsoft Windows XP. Instructions and details for wireless network establishment are included in Appendix F. If wireless network quality is inadequate for control of the data acquisition system, the Remote Desktop Connection function may also be used to established through a wired connection

Battery

An estimated power consumption of 30W will draw approximately 2.5A from a 12VDC voltage source. To deploy the data acquisition system for at least 12 hours without recharging the battery, a battery of at least 30AH capacity is required. A 34AH sealed marine battery was borrowed from a project by Jim Irish for temporary use in with the data acquisition system.

Data Retrieval

Data retrieval from the data acquisition system may be accomplished via a wireless or wired connection to a master computer using the Remote Desktop Connection option on the master computer.

Software

Microsoft Windows XP is installed as the operating system to support a National Instruments data acquisition software package. Remote Desktop Connection software is included with Windows XP, allowing wireless control of the data acquisition system. National Instruments LabVIEW is installed with drivers for the NI USB-9215A ADC. A simple program for data filtering, sampling, and recording may be written in LabVIEW and created as an executable file. For simplicity, this executable may be programmed to run as a scheduled task immediately upon startup by following the instructions outlined under Operating Instructions – Data Acquisition System.

Operating Instructions – Data Acquisition System

Startup

The data acquisition system and hydrophones are powered in parallel by a 12VDC sealed marine battery in series with a marine toggle switch. Start the data acquisition system by switching the toggle switch to the "ON" position. Similarly to a regular desktop computer, the data acquisition system requires a short period of time to boot up before measurements may begin.

Establishment of Wireless Network/Remote Desktop Connection

Once the data acquisition system has been booted, a wireless or hardwired connection may be established with a master computer for control of measurement. Remote Desktop Connection (RDC) software is pre-installed with Windows XP on the data acquisition system, but must be downloaded and installed on the master computer if not already available. Remote Desktop Connection software is available for download at http://www.microsoft.com/windowsxp/downloads/tools/rdclientdl.mspx.

Once the RDC software is available on the master computer, the following directions may be followed to establish a connection with the data acquisition system:

Click **Start** → click **All Programs** → click **Accessories** → click **Communications** → click **Remote Desktop Connection.**

If the data acquisition system wireless network is available, the master computer will detect its presence and allow connection by following the directions below. All computer connection, identification, and security information required for RDC is presented below in Table 1. Information must be entered exactly as it appears in Table 1.

Enter the Internet Protocol (IP) address of the data acquisition system. At the prompt, enter the SSID and WEP KEY.
To terminate the Remote Desktop Connection at the end of measurement, click Start → click Log Off → click Log Off.

Table 2: Wireless networking information for the data acquisition system with a Remote Desktop Connection

Information	Setting
IP Address	10.10.10.1
SSID	BUOY_NETWORK
WEP KEY	abcde
Network Authentication	(open)

LabVIEW Program as a Scheduled Task

Microsoft Windows XP allows scheduling of programs as **Scheduled Tasks** for execution at user-specified times. A LabVIEW executable application may be configured as a Scheduled Task if hydrophone output measurement is desired as quickly as possible after startup of the data acquisition system with minimal LabVIEW setup. The following directions may be followed to schedule a LabVIEW executable as a task in Windows XP:

Click **Start** → click **All Programs** → point to **Accessories** → point to System Tools → click **Scheduled Tasks.**

Double-click **Add Scheduled Task** to start the **Scheduled Task Wizard** → click **Next**.

If the LabVIEW application does not appear in the list of programs available for scheduling, click **Browse**. Click the folder and file for the desired LabVIEW application and click **Open**. Enter an appropriate name for the task, such as "LabVIEW Program 1," then select "When my computer starts" as the time for Scheduled Task execution.

If prompted, enter the user name and password of the data acquisition system, included in Table 1, to run the application as if it were started by that user. Click Next → click Finish.

To remove a Scheduled Task, click **Start** → click **All Programs** → point to **Accessories** → point to System Tools → click **Scheduled Tasks.** Click the name of the Scheduled Task to be removed and click "Delete this item" in the column to the left of the list.

Mooring & Buoy Design

Mooring

The calculations that were done to determine required elasticity of the compliant member can be seen in the FEA analysis section. Average tidal and sea state conditions were taken into consideration when determining the length of the main mooring line as well as the type and length of the compliant member.

The ballast, a series of iron rings weighing is attached to the main mooring line. Three galvanized steel rods hang below the flotation and connect to the mooring line in a triangle basket shape that hangs below the extruded canister. These rods are bolted to the top of the canister and hold the entire system together.

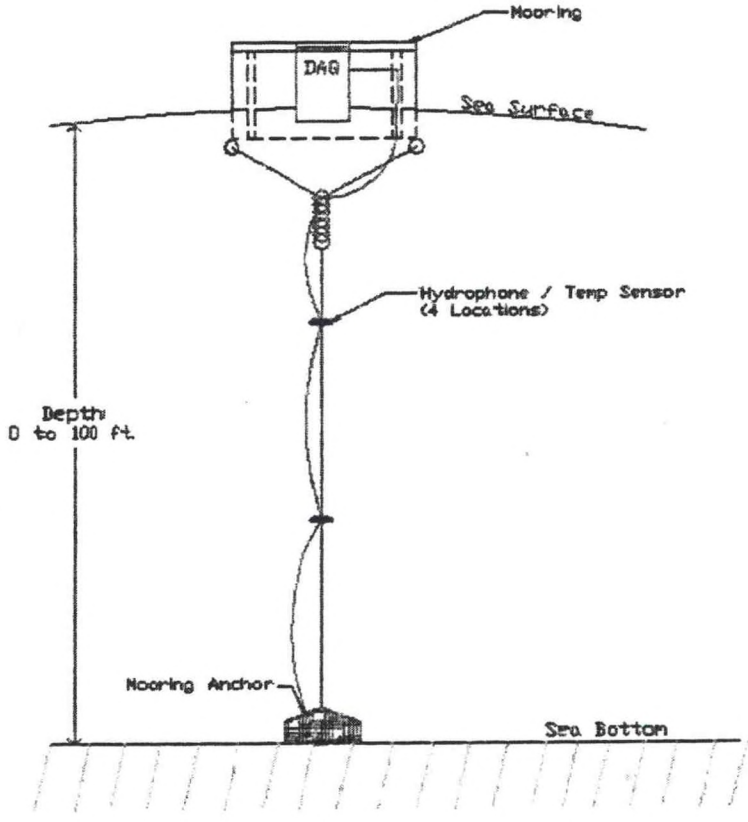

Figure 9: Mooring design with attached buoy and measurement device placements.

Buoy

Instead of purchasing a ready-made piece of floatation, it was decided that a custom-built buoy would more readily suit the demands of the project and cost less. Because the central canister was made to fit the computer system and battery, the buoy was made to fit the canister. Pink polystyrene foam was selected and cut into 36'' rounds. The foam base was covered in fiberglass mesh and coated with epoxy resin. Once dry, the floatation was watertight and could be painted. Since the buoy is to be used for research, yellow

exterior paint was selected in accordance with Coast Guard regulations. The figure below illustrates a design layout for the buoy.

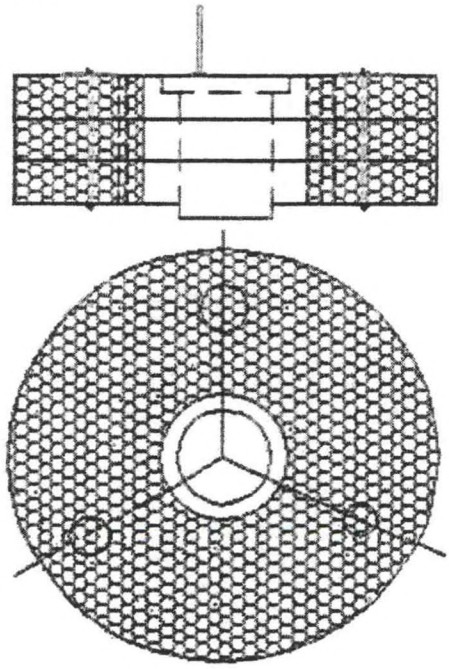

Figure 10: Buoy schematic illustrating dimensions and hole locations as well as canister placement.

Model Fabrication

Buoy Construction

To build the buoy, two-inch-thick pink polystyrene foam sheets were stacked up and glued together with Liquid Nails adhesive. The buoy used five sheets yielding an overall height of ten inches. Outer edges of the buoy were trimmed down to approximately 36 inches in diameter. A central ten-inch-diameter hole was drilled out of the buoy for canister insertion. Three ten-inch-long sections of half-inch-inner-diameter PVC tubing were fitted snuggly into equally-spaced half-inch-diameter holes drilled through the polystyrene. These three fittings serve for holding the half inch diameter steel threaded rods for mooring attachments. A ten-inch-long section of two-inch-inner-diameter PVC was fitted into a final hole drilled out on one side of the buoy; this slightly larger diameter hole will be used to feed data cables from lower mooring attachments up through the buoy to the top lid of the canister with appropriate connectors.

Upon completion of foam construction of the buoy to match specified dimensions, the buoy needed to be sealed water tight. A West System epoxy resin was applied to a layer of chopped fiberglass on all sides of the buoy and central hole before being covered with a second layer of fiberglass mesh cloth. After drying, the buoy edges and fiberglass seams were sanded down and patch work around the smaller holes was completed before a second coat of fiber glass was applied. After completely drying, the buoy was painted with a coat of yellow marine-grade watertight paint for research buoy identification.

Data Acquisition Housing Canister Construction

The canister was built to house the battery and data acquisition system. A 10'' diameter PVC pipe, cut to 22'' in length is used as the main component of the canister. Two end pieces were constructed from PVC plates. The bottom is a sealed, permanent fixture that is glued to the inner diameter of the can with 5200 West System epoxy. The top is a removable lid that is secured with two stainless steel Nielsen clips and kept watertight with a 1'' thick neoprene seal which is compressed when the lid is shut. A 14"-diameter PVC flange is attached to the top end of the canister and allows the can to rest in place within the buoy.

Inside the canister there are two levels for the computer components to reside in. The bottom holds the battery which sits on top of a ½'' neoprene disk to absorb impact stress that occurs on the battery and provide insulation to mitigate thermal stresses in the battery. The main computer assembly is supported by a central divider disk approximately eight inches above the bottom of the canister. The data acquisition system has connections through the top through which the data is relayed. A series of water-tight fixtures allows for on-site data retrieval without the risk of water getting into the canister. The following illustration is a cross section of the housing component with battery and computer spacing.

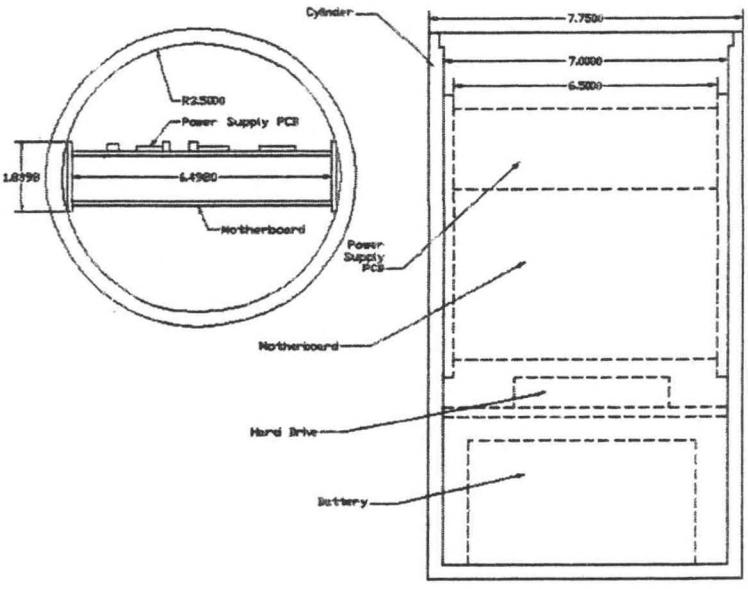

Figure 11: Cross-sectional diagram of internal housing component setup.

Mooring Construction

The mooring line, 70' of ½''thick polypropylene rope, connects to the ballast at the sea floor and to the bottom of the compliant member. The compliant member is elastic and compensates for changing sea surface height.

The buoy is connected to the sea floor with a set of three rods bolted to the top of the floatation. The rods extend through the buoy and past the bottom of the partially-submerged canister. Each of the three rods connects to a short piece of mooring line by a series of D-rings and shackles. This set is connected to the top of the compliant piece, located approximately one meter below the surface. A conceptual schematic of the mooring line arrangement is presented below in Figure 12.

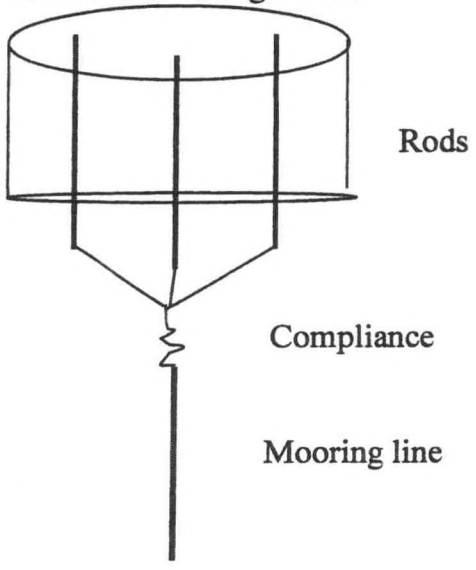

Figure 12: Mooring Attachment

Preliminary Analyses

The following are excerpts from modeling and simulation projects completed to aid in design of the taut mooring system. Simulations were completed by finite element analysis (FEA) in AquaFE/MSC Marc and by state space representation in MATLAB/Simulink.

Finite Element Analysis using AquaFE and MSC Marc

Finite element analysis programs AquaFE and MSC Marc were used during initial buoy design for analyses of buoy dynamics and compliance member selction.

Problem Statement

To measure acoustic effects of pile-driven bridge supports in brackish estuaries, it has been proposed to build a buoy system for acoustic-, pressure-, and temperature-measuring devices, limiting vertical and planar displacements of the instruments for greatest accuracy. To minimize time and expense of building scaled prototypes for in-pool testing, and then full model open ocean testing, it was the objective of this project to use the University of New Hampshire program AquaFE to analytically model a moored buoy system, and define the pertinent parameters of the elastic modulus of the compliant "bungee" cords. These elastic cords are placed in series with the mooring rope to allow for maximum versatility in varying tides, waves and currents, while limiting data errors due to the device displacements and ensuring that sensitive data compilation devices, held within the buoy itself, stays above water. An example of the buoy system can be seen in Figure 13.

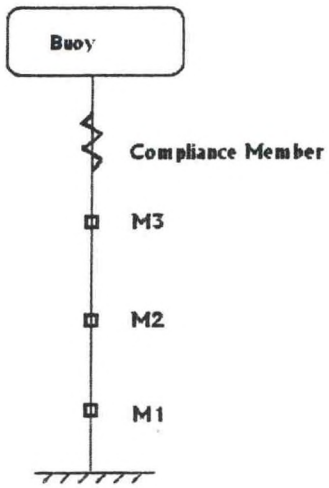

Figure 13: Acoustic buoy mooring setup to be analyzed through FEA methodology.

Analysis

To model the proposed buoy system in AquaFE, as it does not have a graphical user interface, it was first necessary to build a model in a preprocessor that can initialize material properties and boundary conditions. For this purpose MSC Marc Mentat was chosen. The model was built of a single curve of the predetermined height of 12.5 meters. This height was chosen, as it would result in a submerged buoy when moored to the bottom of the proposed application sites in northern Maine and NY, where the buoy would be used. When placed in the ocean, the buoy would be allowed to float to the surface at low and high tide conditions, resulting in enough tension to minimize the buoy watch circle, and movement of the measuring devices in this environment. Nodes were placed at three, six and nine meters to represent, and later monitor, the displacement of the devices that would be placed at these heights, and a compliant member of a lower elastic modulus was placed in between two sections of rope, near the top of the buoy system, to model the "bungee" cords. Finally a "buoy" element was placed at the uppermost section. Figure 14 shows this configuration. After the components were set, the curve was discretized into 10 units per section, and the elements initialized for these units. Fixed displacement boundary conditions were set for the lowest node on the "mooring rope."

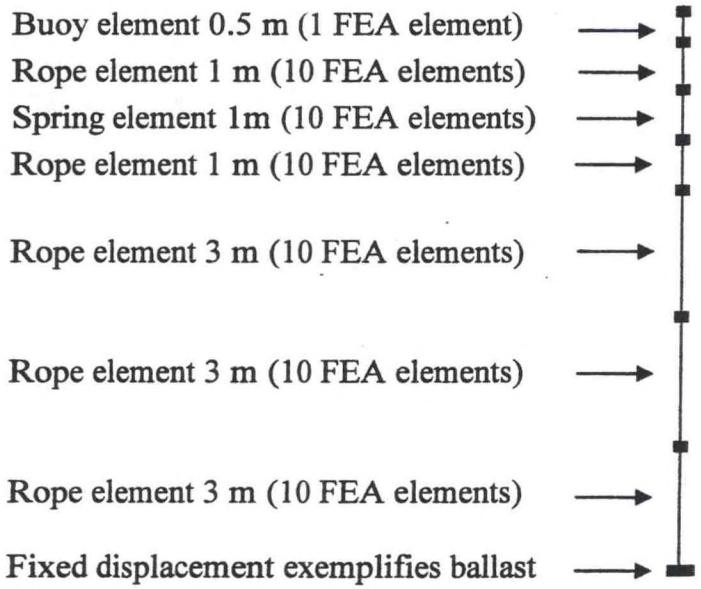

Figure 14: Dimensions of the buoy and FEA model divisions

After the completion of the model, it was saved, and the files converted for use in AquaFE. It is here that the two wave heights with a single wave length and single current with two different tide parameters were added, as well as the material and geometric properties, and the results evaluated and compared for optimization. These values, shown in Table 1, were then run in AquaFE, and the results viewed in Marc/Mentat for a 20000-increment time span. This long duration ensured that the system would reach its steady state position. Competing parameters of increased stiffness of the compliant member to minimize movement, and decreased stiffness to allow the buoy to stay above

water at higher tides, required several iterations before an adequate Young's modulus was reached of 1.0E6 N/m^2.

Analysis Parameters:			**Spring Parameters:**		
Density of water	1025	(kg/m^3)	Young's Modulus	1.0e6	(N/m^2)
Density of surlyn (buoy)	16.06	(kg/m^3)	Cross-sectional Area	0.0003629	(m^2)
Buoy area	0.567	(m^2)	**Tide – Current Parameters:**		
Buoy height	0.5	(m^2)	Low Tide = 13.5 m	Currents = 0.25m/s	
Rope area	3.6e-4	(m^2)	High Tide = 15.5m		
Rope length	12	(m)	**Wave Parameters:**		
Gravity	9.81	(m/s^2)	*Wave – 1*	*Wave – 2*	
Rope area(used in test)	0.049	(m^2)	Height = 0.25m	Height = 0.5m	
			Length = 4.3m	Length = 4.3m	

Table 3: Simulation parameters for finite element analysis

With the above parameters, and knowing that the value for the spring element's Young's modulus was found to be 1.0e6 N/m^2 the spring constant can be calculated using the following equation.

$$k = EA/L$$

Equation 8: Spring constant

Results

When calculating a value from the Young's modulus, using Equation 8 displayed above, the resultant spring constant was found to be 362.9 N/m. Selecting a bungee cord with a spring constant approximately equivalent to this predetermined value for the spring element is essential to compare the simulation results to expected movements of the actual buoy design.

After running various simulations of the model with the AquaFE program, results are obtained that model the dynamic deformation of the buoy when subjected to a current and varying wave conditions over time. The pictures below depict the buoy system's position when it reaches its maximum displacement for each simulation. A total of eight simulations are completed, each displaced under a different parameter for wave input.

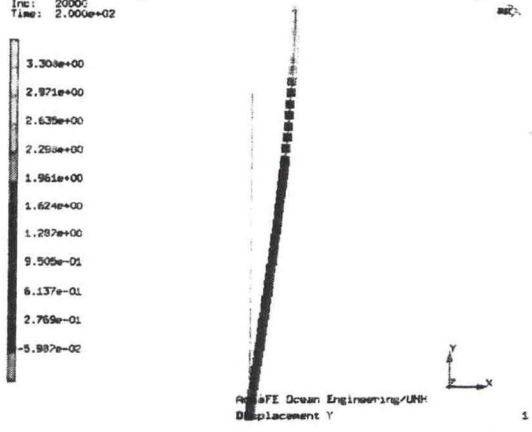

Figure 15: High Tide, High Waves – Y-displacement

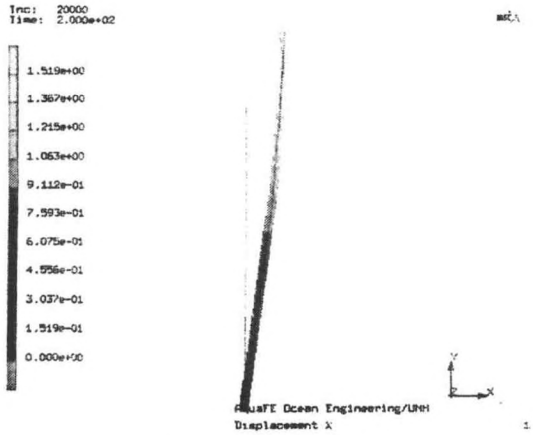

Figure 16: High Tide, High Waves X-displacement

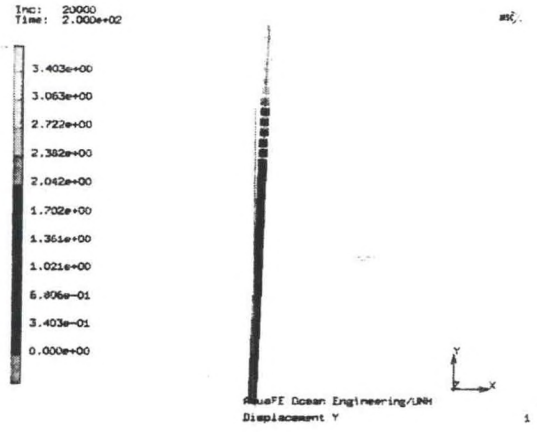

Figure 17: H Tide, L Waves Y-displacement

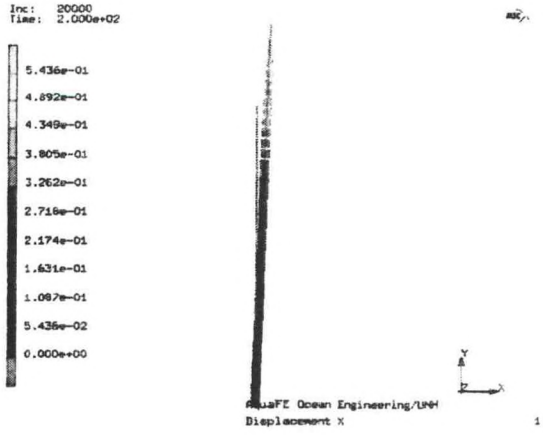

Figure 18: H Tide, L Waves X-displacement

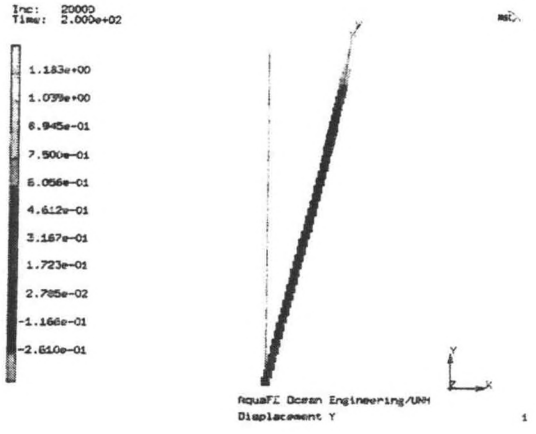

Figure 19: L Tide, H Waves Y-displacement

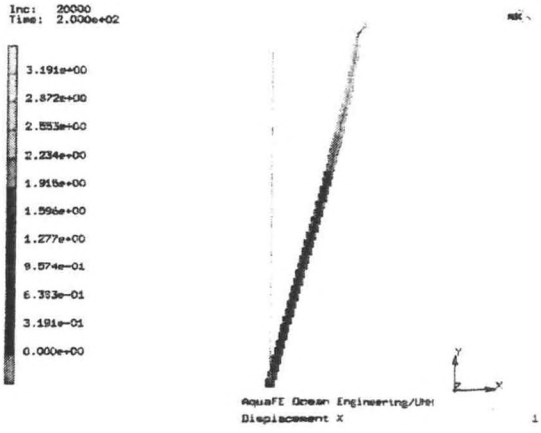

Figure 20: L Tide, H Waves X-displacement

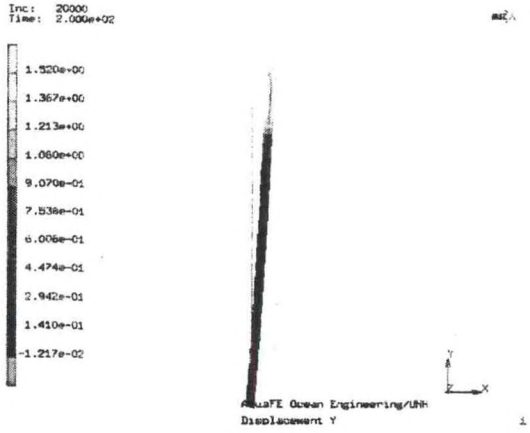

Figure 21: L Tide, L Waves Y-displacement

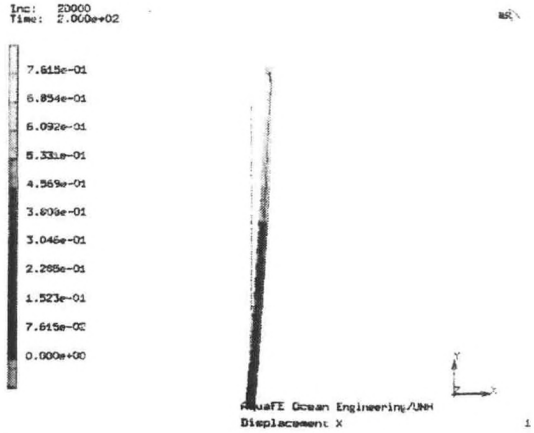

Figure 22: L Tide, L Waves X-displacement

It can be noted that the buoy element, represented by the top element in the models, is straight holding the line quite taut in all the high tidal scenarios as the buoy is partially submerged beneath the surface of the water. Contrarily, in all the low tide cases the top buoy element lies at varying angles to the rest of the mooring line as the water level is lower and the buoy element floats along the surface of the water as it encounters each wave with more play in the spring compensation element.

The AquaFE program can be set up to output the numerical values of displacement of specified nodes and the stresses of desired elements. The table shown below is constructed in a fashion so as to easily compare the max displacements of the nodes at each measuring device from their initial position in both the vertical (y) and horizontal (x) directions.

	Low Tide (13.5m)		High Tide (15.5m)	
	Wave 1	Wave 2	Wave 1	Wave 2
Max X - Displacement (m)				
M1	0.226	0.72	0.145	0.401
M2	0.426	1.41	0.277	0.787
M3	0.605	2.07	0.393	1.15
Max Y - Displacement (m)				
M1	0.007	0.086	0.001	0.024
M2	0.013	0.166	0.002	0.047
M3	0.017	0.238	0.004	0.066

Table 4: Displacement results at the location of each measuring device attachment.

From these results the following table is constructed where the maximum displacements of the measuring devices at a certain tide and wave condition are summarized. The x- and y- displacements are obtained by the difference between the maximum and the minimum nodal displacements. The total displacement is calculated from the x- and y-displacement, using the following equation,

$$\text{Total displ.} = (\text{x-displ.}^2 + \text{y-displ.}^2)^{1/2}.$$

Equation 9: Total displacement

	Low Tide (13.5m)		High Tide (15.5m)	
	Wave 1	Wave 2	Wave 1	Wave 2
Max X - Displacement (m)				
M1	3.91E-02	6.94E-02	4.48E-02	7.12E-02
M2	6.20E-02	1.13E-01	7.99E-02	1.26E-01
M3	8.77E-02	1.52E-01	1.04E-01	1.68E-01
Max Y - Displacement (m)				
M1	2.87E-03	1.67E-02	2.02E-03	9.14E-03
M2	4.52E-03	2.70E-02	3.54E-03	1.61E-02
M3	5.75E-03	3.53E-02	4.49E-03	2.12E-02
Total displacement (m)				
M1	0.039199	0.071365	0.044888	0.07175
M2	0.062211	0.115992	0.079975	0.127054
M3	0.087906	0.156163	0.103772	0.169384

Table 5: Total displacements at each measuring device attachment

The highest displacement is 17 cm; this value is attained at the node in the highest location (M3 in Figure 1). This value could be reduced by implanting the measuring device lower along the mooring cable.

Stress considerations are also analyzed from the AquaFE output file. The following graph displays the stress oscillations in the lower rope element after the spring compensation component.

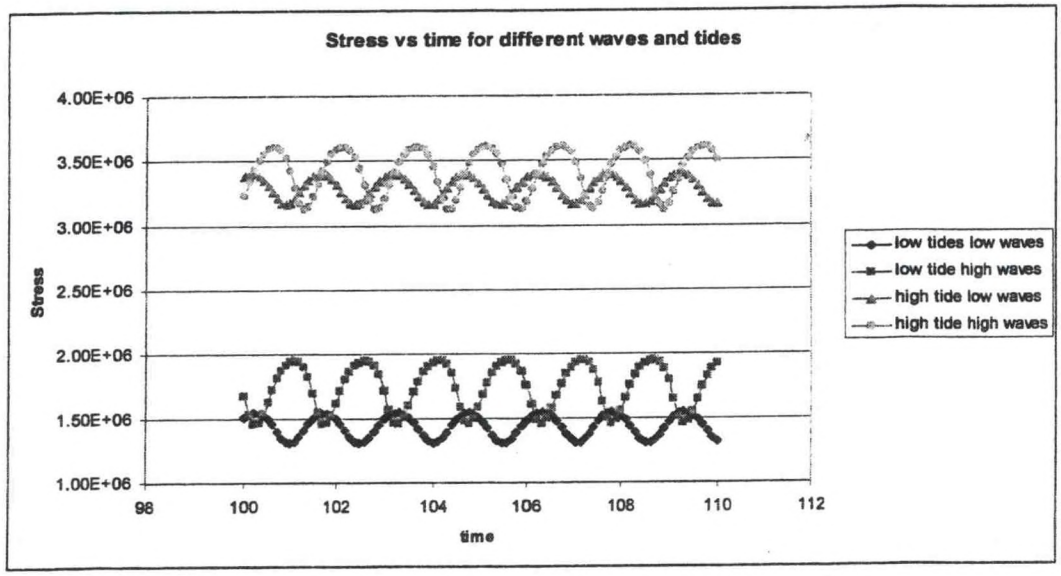

Figure 23: Stress oscillations in the lower Rope element over waves duration.

It can be noted that the stresses are larger at high tides and the oscillations have increased amplitudes with higher waves. The following chart illustrates the maximum stress reached over the wave span for each wave and tidal condition.

	Low Tide (13.5m)		High Tide (15.5m)	
	Wave 1	Wave 2	Wave 1	Wave 2
Max Stress (N/m2)				
Stress	1.54E+06	1.95E+06	3.40E+06	3.61E+06

Table 6: Maximum stresses in the lower rope element.

As expected, the maximum stress is reached, for the high tide, high wave's case. From the maximum value of stress, we can estimate the weight needed for the anchor:

Weight = max stress*rope cross-sectional area/g

Therefore,

(3.61E6 Pa)*(0.0003629 m^2) / g (9.8 m/s^2) =134 kg

According to the results from our model and analysis the ballast should be in excess of 134kg.

Testing

To assure that the FEA program accurately calculates the buoyancy of the partially-submerged buoy, a simple test was conducted. This test was setup in such a way as to completely submerge the given Gilman buoy while applying little to no external forces on it. By attaching the buoy to a simple rope with a neutral density, in this case the same density as the surrounding water, and turning off all wave and current loadings an average stress in the cable element is obtained. From this stress, the tension in the cable element can be determined which should be equal to the surface float buoyancy. A quick hand calculation is an alternative method to determining the force due to buoyancy of the specified buoy as demonstrated in the table below. Finally these two values should be compared to ensure that they are relatively the same value. This will prove that the FEA program has been setup correctly to compensate for the buoyancy.

Hand Calculations for Buoyancy:	**FEA Results for Tension:**
Fbuoy = (density water)*(buoy volume)*(gravity)	Average Stress in Rope Element:
Fbuoy:	57137.46 Pa
2850.663375 (N)	
Wdry = (buoy density)*(buoy volume)*(gravity)	
Wdry:	
44.6650281 (N)	
Buoyancy = Fb-Wdry	**Tension = (Stress)*(Rope Area)**
2805.998 (N)	**2799.74 (N)**

Table 7: Buoyancy Force Calculations

As shown above, it is noted that both methods produce a similar value for the force on the buoy. The FEA program is found to produce a buoyancy that is only 0.2% in error from the theoretically-calculated value for the given buoy parameters.

Conclusions

After becoming acquainted with the AquaFE program, the initial objectives of the finite element analysis were reached. The buoy system was functionally modeled and with expected estuarine conditions applied, a proper stiffness for the wave and tidal compensation component was reached. Based off of planar and vertical displacements in multiple wave environments, with applied low and high tides typical for the estuaries in study, it was found that a compliance member with a spring constant of approximately 360 N/m is adequate for the buoy parameters as previously specified. This value can be adjusted for further analysis with the addition of different wave and tidal conditions.

Applying this value to the model obviously resulted in some displacements, but they are believed to be minimal for the given environmental conditions. The multiple simulations run in AquaFE also produce output values that can be transferred to an Excel file for further analysis. Here, displacements in both directions were assessed over the 20,000 increment wave duration and the maximums selected. Also maximum stresses in pre-selected rope elements were evaluated to determine the greatest tensions the cable member would have to endure.

In conclusion the AquaFE program was found to be quite a challenge at first to understand, but after gaining some familiarity with the program the group began to work more efficiently, identifying errors rapidly as compared to the start. Attached is a guideline with a discussion of some of the problems we continually encountered when using the program that may be of aid to future students learning the program. After completing this project the group feels confident in our abilities to later use this program to further analyze the buoy system at hand or for other ocean engineering applications.

System Modeling Analysis Using MATLAB

Though this analysis was completed for a 500-lb capacity cylindrical Gilman buoy, the results may be applied to the custom buoy of similar shape and orientation so long as the difference in maximum capacity is observed.

Abstract

Wave amplitude and frequency responses of an underwater acoustic measurement system and associated mooring hardware were examined using a MATLAB state-space representation for an extended mass-spring-damper system with a single sea surface height input and fixed ballast. Maximum vertical and horizontal displacements of the main buoy and several hydrophones along the mooring line were plotted versus wave period for multiple wave amplitudes typical of estuarine conditions where such an acoustic measurement system is likely to be deployed. Resonant frequencies were observed for both vertical and horizontal maximum displacement magnitudes, with relatively great overshoot values observed. Minimal damping effects in the mooring system were determined to yield a nearly-negligible damping coefficient, producing such substantial magnitude results at the resonant frequencies. Buoy drag coefficient parameters were to be determined experimentally; time constraints and experimental difficulties forced the use of a researched theoretical drag coefficient value for simulation purposes.

Objective

The objective of the experiment and analysis was to determine optimal tidal compliance parameters of the given buoy system shown in Figure 24 below. Modeling of the buoy and remainder of the measurement system response to varying wave frequencies and amplitudes was intended to aid in the optimization of tidal/wave compensation design in the mooring system. Because hydrophone movement is detrimental to the desired accurate measurement of underwater noise, this project focused on simulation of hydrophone movement for a range of wave conditions. To properly model the buoy system, several measurements were required, including mooring line elasticity and damping coefficient, masses and buoyancy properties of various components.

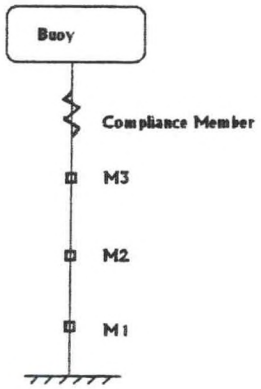

Figure 24: Schematic of buoy design to be modeled

In short, this experiment was intended to determine the following results for the schematic shown in Figure 1:

- Vertical and horizontal displacements at intervals along the mooring system where measuring devices are located (M1, M2, M3), for a multitude of varying wave frequencies
- Development of guidelines for potential compliance member design
- Experimental determination of the drag coefficient of a selected buoy over a range of potential river conditions

Introduction

A taut-moored buoy system will be used in an underwater acoustic measurement arrangement. A common 500 [lbf] buoyant cylindrical buoy, supplied by Gilman Corporation, is used to house a data acquisition device housed within a central drilled hole. Attached to this buoy, through the use of a bridle, is a mooring cable which spans a short distance through the water to a compliance member. This compliance will be obtained through the use of several elastic cords secured in a fashion to obtain the desired mooring tension during deployment. A second, longer cable is coupled to this elastic cord and spans the local depth to the estuarine floor where a large weight is used as ballast. At equivalent distances along this lower cable, three stations comprised of multiple measuring devices including hydrophones are affixed.

It is essential to note the importance of the compliance member in the taut mooring system. The compliance of this member is dependant on the wave, current and tidal conditions of the specified estuary. For the purpose of this design, our buoy will be deployed into rivers with relatively low currents, wind speeds not exceeding 4 knots, little to no tidal changes and an average depth of 10 to 40 meters. A compliance member is selected to optimize the mooring system design, while keeping the line taut in any potential estuarine conditions that would fall within the allotted parameters of the researched rivers.

Analysis

A MATLAB state-space representation method was chosen for two-dimensional modeling of the buoy and taut mooring system. Equations of motion were developed for all points of interest along the taut mooring line using a simplified, but extended, mass-spring-damper system approach and assuming fixed ballast. Figure 25 depicts a schematic of the points considered for vertical equations of motion, and indicates the variable buoyancy forces induced by changes in sea surface height. In the vertical model, buoyancy force was defined as the difference between buoy weight and the weight of estuarine water displaced by the buoy having a known cylindrical cross-sectional area and submergence dictated by sea surface conditions.

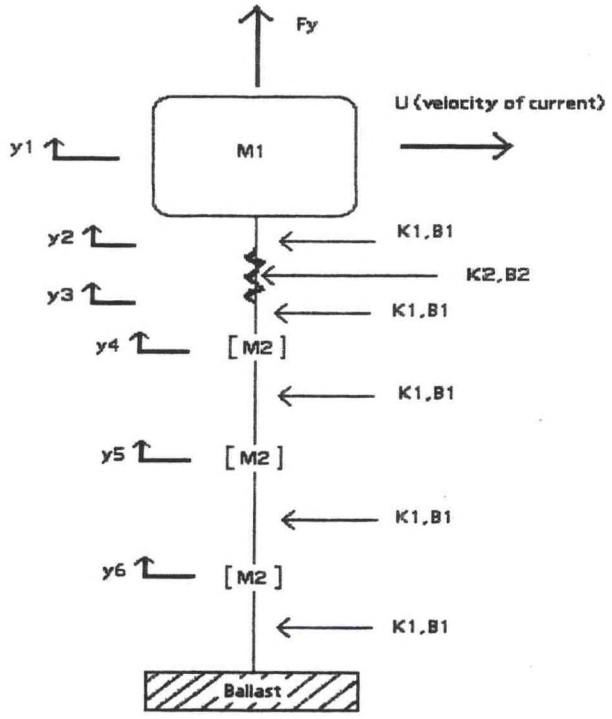

Figure 25: Schematic for vertical system analysis for vertical displacement to determine state space representation for MATLAB model.

Horizontal equations of motion were developed in a similar fashion, though buoyancy forces were replaced with viscous and stagnation drag forces induced by a constant current, calculated using Equation 10, below. Drag force in the state-space model was defined as the product of multiple parameters, the most variable of which was the submerged buoy cross-sectional area in the direction of flow. Holding the buoy radius constant, cross-sectional area for drag calculation was defined as the product of the buoy radius and the buoy submergence depth. Drag force, F_{drag}, was calculated according to

$$F_{drag} = \frac{1}{2} C_d \rho A U^2,$$

Equation 10: Force of drag

where C_d is the object drag coefficient in a particular medium (in this case, seawater), ρ is the medium's density, A is the cross-sectional area in the direction of flow, and U is the flow velocity. Drag and buoyancy forces are thus somewhat coupled by their interdependence on buoy submergence, itself a function of sea surface height and buoy state. Several experiments to determine drag coefficient of the buoy were attempted before a theoretical result, based on research of buoys with similar shape and size, was selected for use in the MATLAB model. A table of all system parameters relevant to the state-space model is presented below in Table 8.

Component	Parameter	Value
Buoy	Mass	30 [kg]
Buoy	Drag Coefficient	0.63 [-]
Buoy	Cyl. CS Area	0.5 [m^2]
Hydrophone	Mass	2 [kg]
Compensation	Spring Constant	50 [lbf/ft]
Compensation	Damping Coefficient	10 [lbf-s/ft]
Mooring Line	Spring Constant	10 [N-s/m]
Mooring Line	Damping Coefficient	1 [N-s/m]
Mooring Line	Length	40 [m]
Estuary	Depth	40 [m]
Estuary	Current	1 [m/s]
Estuary	Seawater Density	1015 [kg/m^3]
Estuary	Wave Amplitude	0.25, 0.5, 1 [m]
Estuary	Wave Period	0.25 - 5 [s]

Table 8: System parameters used for state-space representation

Several deficiencies of the model result immediately from the chosen simplifications made during state-space development. Particularly, distributed loading due to mooring line and compensation member masses were neglected. Also neglected were drag effects on each hydrophone package. Hydrophone package weights were considered, effectively yielding buoyancy and drag forces on the buoy as primary inputs to an extended mass-spring-damper system.

MATLAB state-space results include maximum vertical and horizontal displacements for the buoy and each hydrophone package for wave amplitudes of 0.25, 0.50, and 1 [m] with periods ranging from 0.25 to 5 [s]. Simulation results clearly indicate wave periods for which vertical and horizontal displacements exhibit theoretical maximums.

Experimental Methodology

To determine the drag coefficient of the group's specified buoy, shown below, an experiment was arranged to utilize the long wave tank in the Chase Ocean Engineering Laboratory. To determine the drag coefficient, the buoy was dragged by a load cell through water at varying speeds with varying buoy depths to determine the force required for steady-state velocity. A final drag coefficient was to be determined by averaging the experimentally-determined drag forces over a variety of velocities and submergences.

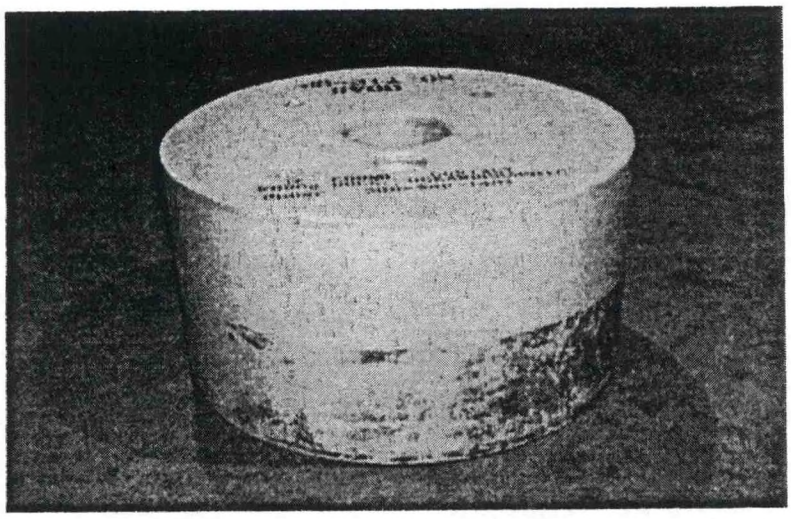

Figure 26: Gilman Corporation's buoy: to be used in drag experiments.

A pulley system was arranged that would attach to the moving platform in the wave tank. This pulley device extended to just below the water's surface to minimize the angle at which the extended line pulled the buoy. Pitch, roll, and heave angles may be neglected for adequately-horizontal pulling line angles. The constructed towing setup is shown below.

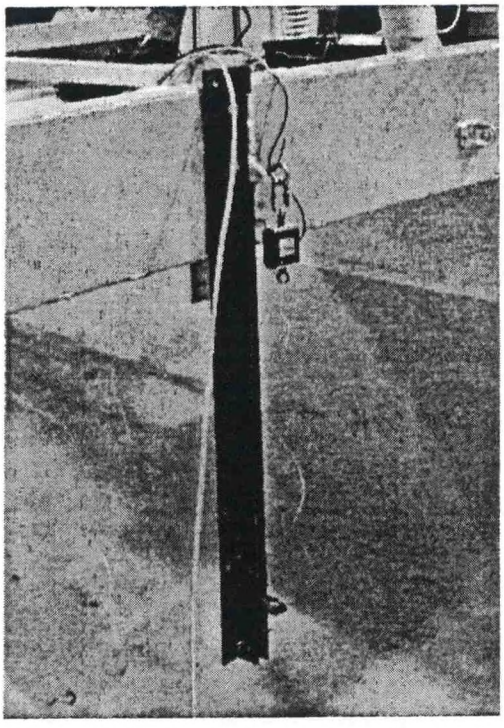

Figure 27: Constructed experimental setup to drag buoy via pulley with attached strain gauge load cell. The light white wire tied to the load cell is 100lbf-rated monofilament.

A 100lbf-capacity monofilament nylon wire was looped through the pulley before being knotted to a 112lbf-capacity tension strain gauge load cell.

After adjusting the stationary equipment to the platform, the buoy was affixed. The monofilament was extended approximately 10 feet to ensure minimal angular changes from the horizontal pulling position, and tied to 65lbf-rated fishing wire before looping the buoy multiple times to distribute the tension forces. This wire was wrapped two inches above the buoy bottom surface, the level at which the unloaded buoy rests in the water.

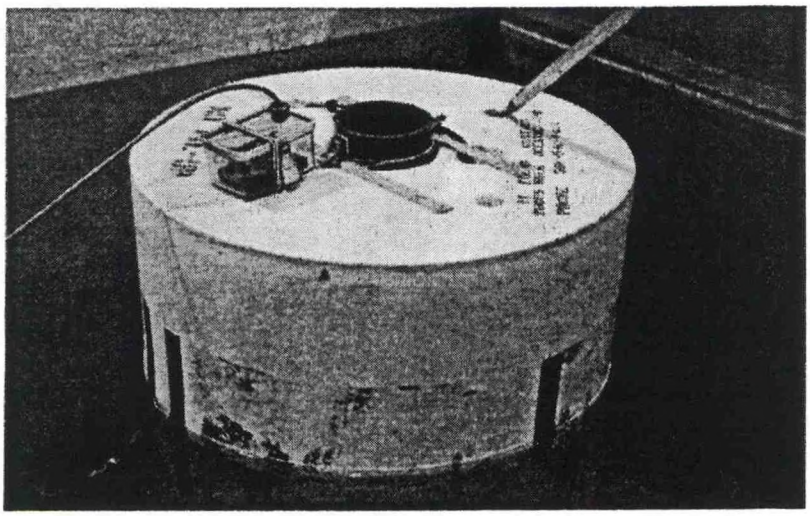

Figure 28: Gilman buoy prepared for experiment with attached pitch, roll and heave sensor, and attached to monofilament line with wires wrapped at natural water displacement level.

To ensure that the pull angles occurring during the initial tug were minimal and therefore negligible in drag coefficient calculation, a second measurement device was placed atop the buoy to measure pitch, roll and heave which would occur as the buoy was towed through the tank

A second setup was also used to test drag forces with numerous loads applied to the buoy. To accomplish this, weights were attached to the top of the buoy to simulate loadings of 0lb, 30lb and 60lb. To attach these weights, a grate was set atop the buoy, attached through the drilled holes, and lead weights were secured across the grate. With the addition of weight, the buoy sunk slightly in the water, increasing the submerged surface area perpendicular to flow direction

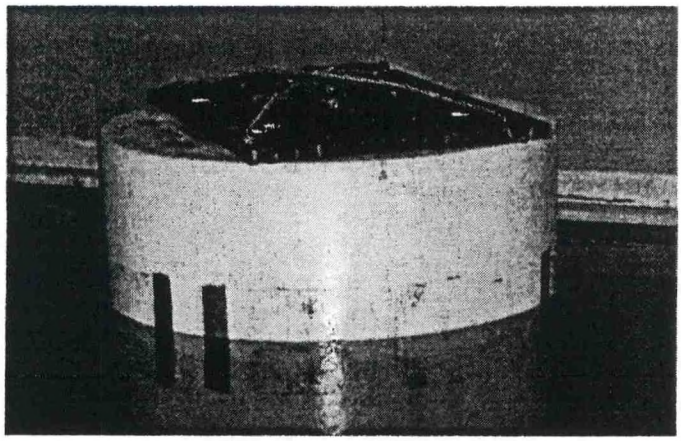

Figure 29: Buoy with attached grate and 60lb lead weight load secured across the grate.

After completing all the experimental setups, multiple tests were attempted. Runs were intended to be completed to record the force of drag from the load cell for buoy loads of 0lb, 30lb and 60lb over velocities of 1 knots, 2 knots and 3 knots. From these nine runs, assuming no equipment malfunction or wave tank operator error, the results would be sufficient to determine the coefficient of drag for the specified buoy to use in the MATLAB analysis.

Results

Experimental Results

The experimental determination of the drag coefficient for the buoy did not go as smoothly as anticipated. Over a three-day time span, approximately 15 hours in the OE lab, numerous problems were encountered. The first setback occurred during a tow of the buoy up to a speed of two knots, resulting in failure of the monofilament-to-fishing wire connection. This would not have been a great problem, except that the buoy lurched in its own wake and capsized, allowing the grate and full loading of lead weights to sink, as seen in Figure 30.

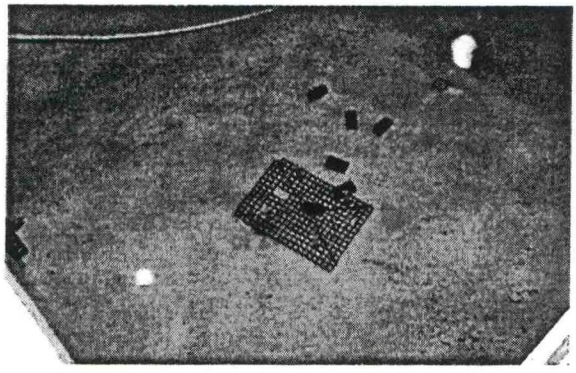

Figure 30: Sunken grate and lead weights after monofilament failure and capsizing of buoy

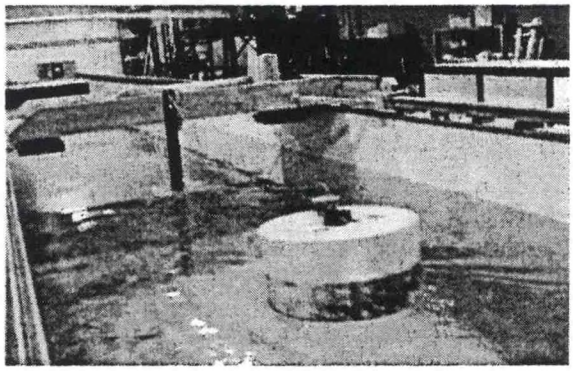

Figure 31: Test drag run of the unloaded buoy in the wave tank at minimal velocities

With this minor setback, and no one caring to don wet suits for the day, it was decided to attempt unloaded buoy tow runs at varying speeds. This process worked well during several test runs without the load cell. However, once Prof Andy McClaugh (the licensed operator of the wave tank equipment) attempted to make a drag run while recording the drag forces from the buoy, a hardware failure occurred in the load cell signal conditioning equipment. Long hours and multiple other runs repeatedly resulted in the same fashion. Problems with hardware, recording software, computer malfunctions, operation equipment or snapping towing lines repeatedly caused test data to be lost.

After multiple failed attempts and a discussion with professors assisting with the experiment, it was decided to use drag coefficient data from Berteaux's text *"Coastal and Oceanic Buoy Engineering"* for a buoy with the experimental buoy dimensions and shape. This research yielded a drag coefficient of 0.63 [-].

Analysis Results

Simulation of vertical and horizontal displacements was performed for each hydrophone package for varying wave amplitudes with zero tidal input and 1m/s current. The buoy was analyzed for .25 m, .5 m and 1 m wave amplitudes. Figure 32 shows the maximum horizontal displacement versus wave period for a wave amplitude of 0.25 m. Similar plots for .5 m and 1 m wave amplitudes are included in Appendix D.

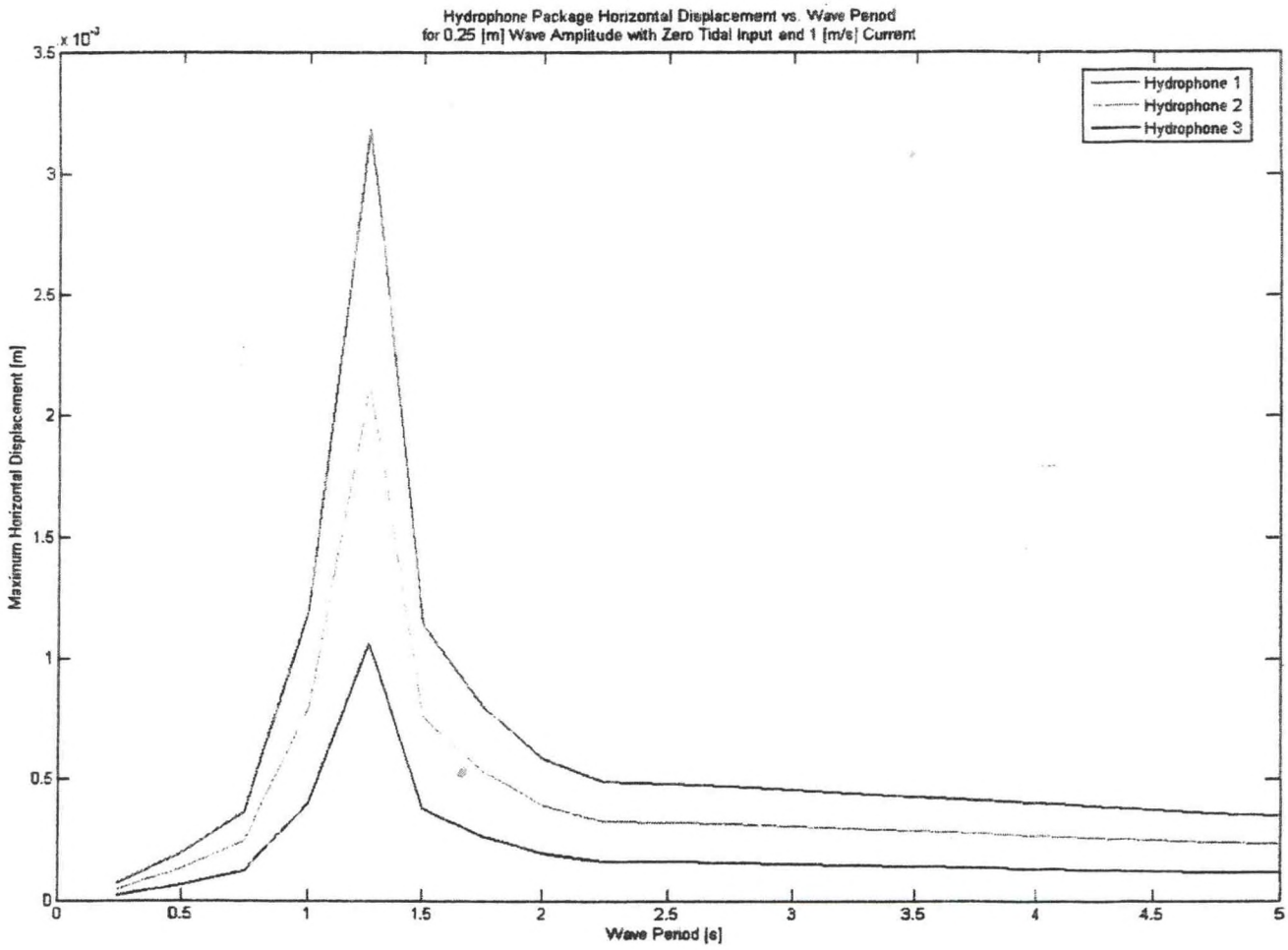

Figure 32: Maximum horizontal displacement versus wave period for .25m wave amplitude

Because buoy displacements occurred on a relatively great scale compare to hydrophone displacements, buoy response was plotted separately from hydrophone package response. Figure 33 depicts buoy horizontal displacement for three different wave amplitudes. Similarly, figures in Appendix D present the maximum vertical displacements for the hydrophone packages and buoy for all ranges of wave frequency and amplitude.

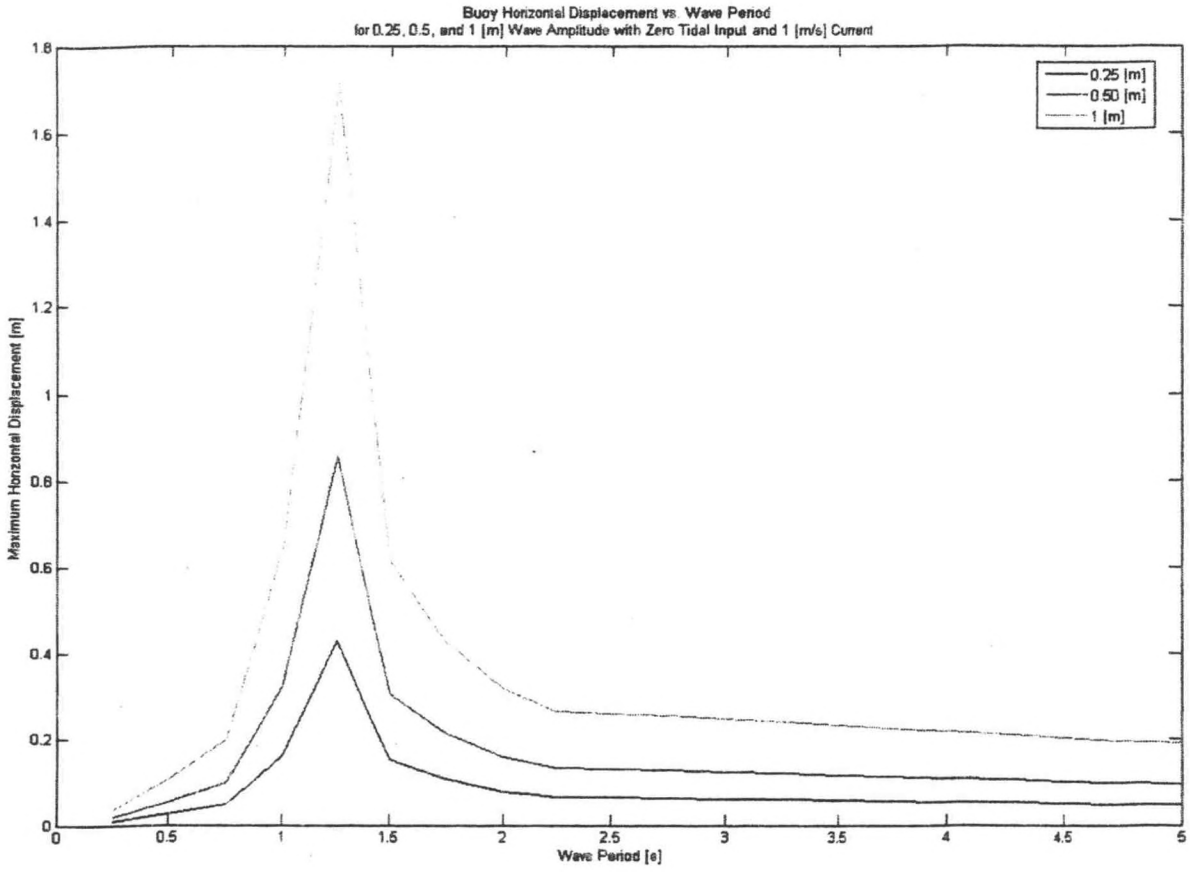

Figure 33: Buoys horizontal displacement versus wave period for varying wave amplitudes

Discussion of Results

The scope of this experimental exercise took many forms over the course of theoretical, experimental, and analytical development. Initially, this project was designed to model an underwater acoustic measurement buoy and mooring system with the purpose of determining ideal parameters pertaining to tidal and drag force compensation elements and reduction of detrimental hydrophone motion. Tidal, wave, and current inputs were identified as the most important driving forces; responses of the mooring system to fluctuations in each input were desired for a range of mooring compensation spring constant values. Because the modeled system is a real-world design intended for manual deployment from a vessel of opportunity, the physical effort required for deployment was also considered, with respect to required ballast and associated parameters. It was quickly discovered that a thorough analysis encompassing the entire original project scope would require far more time and resources than presently available. As such, the more focused goal of system response simulation for ranges of wave frequency and amplitude was chosen with the intention of better understanding the mooring system frequency response in general and individual hydrophone displacement in particular. Additionally, a buoy drag coefficient was to be determined experimentally; it may be noted here that, due to time constraints after repeated experimental attempts, a researched theoretical result was instead employed in the simulation.

A state-space representation was selected for simulation of vertical and horizontal motion of several key elements of the mooring system, including the buoy and each hydrophone package. State space representation was chosen for simplicity of system parameter definition/alteration and the resulting increases in control over all aspects of simulation. However, several system parameters were neglected during model simplification, necessitated mostly by the state-space format which allowed only a single input function. Sea surface height relative to buoy and mooring system equilibrium as a sinusoidal input was selected as the critical driving element, with buoyancy forces and drag forces both defined as functions of differences between sea surface height and buoy state. Several ten-second simulations were completed with wave amplitudes of 0.25 m, 0.50 m, and 1.0 m with wave periods ranging between 0.25 s and 5.0 s. Many estuaries, including the mouth of the Piscataqua River in Portsmouth, New Hampshire, frequently experience such ranges of wave parameters, often with high-frequency, smaller breeze-driven waves and longer storm-driven swells occurring simultaneously. While hydrophone velocity fluctuations (and resulting Doppler shift phenomena) are most detrimental to accuracy of underwater acoustic measurements, the maximum vertical and horizontal displacements are also of concern in determining accurate distances between measurement sites over various tidal and current cycles. Maximum vertical horizontal displacements were calculated and plotted versus wave period for each simulation with varying wave amplitude. It must be noted that the simulation results are purely theoretical, and that ocean engineering conventions of plotting magnitudes versus wave number (period) were followed during the final stages of simulation.

As expected of any extended mass-spring-damper system, maximum displacement varied considerably with input amplitude and frequency. Most notably, an apparent resonant frequency was observed for both vertical and horizontal motion, with rapid magnitude decay at greater frequencies (or shorter wave periods). The observed maximum overshoot which occurs at the resonant frequency above the steady-state displacement value for long wave periods is due to the nearly negligible damping effects included in the simulation. Because mooring line and compensation damping coefficients were determined to have relatively small magnitudes, the net damping constant scales as nearly zero and yields a nearly-infinite magnitude at the resonant frequency. Although in most cases the theoretical maximum displacements greatly exceed the physical limitations of the real-world system, the results may be used to verify general frequency response characteristics of the system. Arranging any of the maximum displacements versus frequency rather than wave period, the resulting plot loosely resembles a Bode diagram for a simple mass-spring-damper system with a damping constant of nearly zero.

While no guidelines for tidal compensation selection were developed, and no successful experimental drag coefficient values were calculated, this project served as an extensive modeling exercise which relied heavily on outside mooring research and careful simplification of the mechanical system. Considering the expected frequency response of the mooring system, the simulation results are easily confirmed qualitatively and may be used to further the understanding of detrimental hydrophone motion for a variety of estuarine or sea surface conditions.

Future Testing

Upon completion of construction field testing will commence. Initial tests will be run in order to calibrate the sensors with the data acquisition system. Using the data from the sample locations, current marine construction projects will be looked into for on-site sampling. The following is an outline for furthering this project.

Calibration

Using a calibrated source transducer and calibrated hydrophone, the hydrophones constructed for this project will be tested and calibrated in the Chase Ocean Engineering Laboratory deep tank.

Programming

LabVIEW programming for the data acquisition system must be completed. A simple program to run the NI USB-9215A ADC, sample, and store data from three analog inputs will be sufficient for basic field testing. Programming for highly-automated "plug-and-play" operations of the data acquisition system should be the focus of future work for this project.

Field Tests

Two field tests are recommended for the initial use of the buoy system. After each part is calibrated the entire system should be assembled and deployed in a controlled tank environment. A calibrated source should then be used to simulate a low-amplitude pile strike, which is to be received, sampled, and stored by the hydrophones and data acquisition system. Analysis of the received data should be done to ensure that all systems are working properly.

The second of the tests should be done in a bridge construction environment. A GPS system can be used to measure the distance between the pile that is being driven and the buoy. Once the buoy is deployed, it should be left to observe for one hour. Data can then be extracted from the canister through the wireless connection and analyzed via a lap top computer.

Bubble Curtain Testing

Once confidence in a working system is established, observations should be done in marine construction environments. "Bubble curtains" around the driven pile have been proposed as viable solutions to attenuate the dangerous levels of acoustic pressure. The buoy system can be used to observe SPL at distances from the source as the bubble curtain is being used. Results from the bubble curtain sites can then be compared to similar sites that did not enlist the use of pressure dissipating devices. Suggestions for the use and future developments of such devices can then be made.

APPENDIX

Appendix A – Guidelines for use with the AquaFE Program

A little awkward!

The hardest part of the program is assessing your errors, there is no output to tell you where errors may lie, it doesn't even mention that an error was encountered, you simply don't get new results, and therefore knowing where most errors tend to happen is pertinent.

1- Creating the Mentat model

To open Marc/Mentat type in the Unix command window: "mentat2005&" (the "&" sign will allow for Mentat to stay open in the background)

• Mesh generation: build your model

Don't forget to sweep! (Delete the extra nodes created when subdividing the elements) One extra node will carry through as an error in both your mesh generation and .opt file.

• Material properties

Just create the properties names, select isotropic and apply them to the corresponding elements. Don't enter any values.

• Boundary conditions

Just the anchor point (fixed displacement)

SAVE the model as a .mud file and WRITE it as a .dat file

2- Converting the MARC input file into AquaFe mesh description

Type in the unix command window: "preaquafe yourfile.dat yourfile.out yourfile.ren"

- Whenever you make even the slightest change to your Mentat model ***DO NOT FORGET*** these two steps:
  1. WRITE your file and immediately after,
  2. Enter the "preaquafe" command in the UNIX operator box.

  Without completing both of these steps your file will continue to run with you old model and make you think that it is just not noticeably affecting your results.

3- Preparing AquaFE input file

Type in the unix command window: "nedit feap.in"

Replace the existing content by:

Yourfile.opt

Yourfile.res

- Every time you create a new file you wish to run you must change the feap.in file. There can be only one feap.in file in your directory when running AquaFE so you must edit it each time.

Close the window

4- Preparing AquaFE file

The format of this file is very important and every space should remain the same.
So we work from an already existing file.
To recall this file type in the unix command window:
"cp /usr/local/aquafe/standard.opt yourfile.opt"
Then open or edit this file by typing in the unix command window: "nedit yourfile.opt"
Modify this file to your parameters (material properties, waves, current...).

- Keeping the .opt program file perfectly aligned with the precise amount of spacing is initially a difficult task, but it gets easier. Whenever you change a number make sure to quickly count or check by eye that the spacing and alignment did not change.
- When adding extra elements to the .opt file it is easy to copy paste an extra line space inadvertently. *This will crash the program.* After editing the elements section place your cursor at the end of each line and delete extra spaces between characters and/or lines.
- A quick way to check the number of nodes and elements your model uses so you can input them to your .opt file is under *Mesh Generation -> Renumber*, don't waste your time counting them all on the screen.

Spring and buoy element are taken as AquaFE rope element with adequate mass density, Young's modulus and cross sectional area. (AquaFE Buoy element is designed for a spherical buoy and the parameters to input are different).

The AquaFE file can also give numerical values for displacements and stresses.
Below in the file you find *hist stress* and *hist disp*. The number next to *hist stress* is the element number where the stress is recorded. By copy and paste you can add as many elements as you wish.
Next to *hist disp* the first number stand for the node and the second for the direction of the displacement (1=x, 2=y, 3=z). By copy and paste you can add as many nodes as you wish.

- When adding lines to the code for what values to output to the histfile, note the order you place them in, for this is the order they shall be displayed in the output, there will be no labels.

Nodes and element numbers can be obtained from Mentat, *mesh generation -> element or node -> show.*
Save and close the window

5- Run AquaFE

Type in the unix command window: "aquafe"

If AquaFE takes less than a second to run, chances are the program crashed somewhere.

6- View results

In the Mentat window, *results -> open -> feap.t19 -> monitor ->def & original*

7- View numerical values

Type in the unix command window: "hist2txt histfile yourfile_data.txt 10"
The number is for the time division, here 10 will give you value for each $1/10^{th}$ of a second.
Open ftp explorer, open yourfile_data.txt. Copy the values onto an excel spreadsheet.
Select first row and perform Data -> text to column -> separated by semicolon.
The data are obtained as follows in the order you entered them in the .opt file

time	Element stress	Node displacement		
		x	y	z

Appendix B – Hist file example: Low tide low wave's case

		Stress in element						Displacement at node			
	Rope 1	Rope 2	Rope 3	Spring		M1		M2		M3	
time						x	y	x	y	x	y
0.01	161.09	242.67	282.987	119681		2.57E-05	1.36E-07	2.57E-05	2.88E-07	2.58E-05	4.7(
0.1	420154	425959	428002	720154		0.000847	0.000352	0.000847	0.000705	0.000852	0.(
0.2	2.53E+06	2.53E+06	2.53E+06	2.47E+06		0.004491	0.002118	0.004605	0.004241	0.004746	0.0(
0.3	3.95E+06	3.94E+06	3.94E+06	3.80E+06		0.007533	0.003297	0.010358	0.006601	0.010519	0.0(
0.4	3.92E+06	3.92E+06	3.92E+06	3.76E+06		0.009316	0.003272	0.014963	0.006553	0.015513	0.0(
0.5	2.50E+06	2.50E+06	2.50E+06	2.37E+06		0.011304	0.002074	0.017337	0.004163	0.018272	0.0(
0.6	504846	510495	512818	764570		0.013916	0.000389	0.019981	0.000806	0.021364	0.0(
0.7	598727	604331	606684	858269		0.018267	0.000437	0.024547	0.000933	0.026199	0.0(
0.8	2.37E+06	2.37E+06	2.37E+06	2.27E+06		0.022322	0.001901	0.030022	0.003879	0.031046	0.0(
0.9	3.35E+06	3.34E+06	3.34E+06	3.21E+06		0.02114	0.002729	0.033227	0.005506	0.034461	0.0(
1	3.11E+06	3.11E+06	3.11E+06	2.98E+06		0.019147	0.002545	0.031778	0.005124	0.039544	0.0(
1.1	1.76E+06	1.76E+06	1.76E+06	1.71E+06		0.018387	0.00142	0.032308	0.002863	0.042169	0.0(
1.2	566772	573425	576360	878055		0.020455	0.000404	0.035203	0.000843	0.045518	0.0(
1.3	1.62E+06	1.62E+06	1.62E+06	1.65E+06		0.024606	0.001254	0.03967	0.002575	0.051528	0.(
1.4	2.81E+06	2.81E+06	2.81E+06	2.72E+06		0.026987	0.002235	0.044805	0.004539	0.060606	0.0(
1.5	2.96E+06	2.96E+06	2.96E+06	2.83E+06		0.026989	0.002358	0.050421	0.004745	0.069631	0.0(
1.6	2.03E+06	2.03E+06	2.03E+06	1.94E+06		0.028896	0.001566	0.054818	0.003158	0.0773	0.0(
1.7	911239	916881	919003	1.19E+06		0.032818	0.000583	0.059347	0.00123	0.08492	0.0(
1.8	1.69E+06	1.69E+06	1.69E+06	1.69E+06		0.03732	0.001181	0.065555	0.002464	0.093071	0.0(
1.9	2.44E+06	2.44E+06	2.43E+06	2.35E+06		0.040093	0.001774	0.072654	0.003639	0.100471	0.0(
2	2.28E+06	2.28E+06	2.28E+06	2.17E+06		0.041732	0.001623	0.07818	0.003314	0.102347	0.0(
2.1	1.31E+06	1.31E+06	1.31E+06	1.36E+06		0.044327	0.000772	0.079406	0.001665	0.102124	0.0(
2.2	1.04E+06	1.04E+06	1.04E+06	1.21E+06		0.047386	0.000493	0.080552	0.001179	0.103231	0.0(
2.3	1.83E+06	1.83E+06	1.82E+06	1.75E+06		0.049199	0.001124	0.082521	0.002468	0.105061	0.0(
2.4	1.95E+06	1.95E+06	1.95E+06	1.86E+06		0.048153	0.001246	0.083565	0.002668	0.104511	0.0(
2.5	1.36E+06	1.36E+06	1.36E+06	1.36E+06		0.04697	0.000775	0.082675	0.001703	0.105003	0.0(
2.6	1.09E+06	1.09E+06	1.09E+06	1.24E+06		0.047573	0.00053	0.082334	0.001237	0.106715	0.0(
2.7	1.74E+06	1.73E+06	1.73E+06	1.66E+06		0.048581	0.001058	0.083766	0.002304	0.107802	0.0(
2.8	1.79E+06	1.78E+06	1.78E+06	1.70E+06		0.048285	0.001107	0.08446	0.002382	0.110797	0.0(
2.9	1.29E+06	1.30E+06	1.30E+06	1.39E+06		0.048033	0.000697	0.085112	0.001551	0.115329	0.0(
3	1.52E+06	1.52E+06	1.52E+06	1.52E+06		0.048771	0.000874	0.087593	0.001896	0.120264	0.(
3.1	1.77E+06	1.77E+06	1.77E+06	1.69E+06		0.049921	0.001069	0.090587	0.002277	0.130244	0.0(
3.2	1.43E+06	1.43E+06	1.43E+06	1.47E+06		0.051138	0.000759	0.095608	0.001626	0.138907	0.0(
3.3	1.47E+06	1.47E+06	1.46E+06	1.48E+06		0.053356	0.000752	0.102945	0.001569	0.142288	0.0(
3.4	1.61E+06	1.61E+06	1.60E+06	1.54E+06		0.057561	0.000794	0.107188	0.001727	0.147003	0.0(
3.5	1.31E+06	1.31E+06	1.31E+06	1.37E+06		0.061303	0.000468	0.109496	0.001175	0.154208	0.0(
3.6	1.40E+06	1.39E+06	1.39E+06	1.38E+06		0.06323	0.000498	0.114196	0.001234	0.159519	0.(
3.7	1.36E+06	1.36E+06	1.36E+06	1.33E+06		0.064438	0.000442	0.118934	0.001082	0.163121	0.0(
3.8	1.22E+06	1.22E+06	1.22E+06	1.27E+06		0.06644	0.000286	0.122573	0.000781	0.162706	0.0(
3.9	1.34E+06	1.34E+06	1.34E+06	1.31E+06		0.068655	0.000337	0.124321	0.000943	0.162018	0.0(
4	1.26E+06	1.26E+06	1.26E+06	1.28E+06		0.070341	0.000231	0.123936	0.000806	0.161528	0.0(
4.1	1.32E+06	1.32E+06	1.32E+06	1.33E+06		0.070711	0.00027	0.124018	0.0009	0.157426	0.0(
4.2	1.40E+06	1.40E+06	1.40E+06	1.39E+06		0.070069	0.000354	0.123033	0.001057	0.155006	0.0(

4.3	1.39E+06	1.39E+06	1.39E+06	1.41E+06		0.069229	0.00036	0.120528	0.001077	0.151542	0.0

Appendix C – MATLAB Program

```
% ME747 Experimental Measurement and Modeling of Complex Systems
% Buoy/Mooring Model Final Project - Stott, Risso, Jerram
% State Space Representation

% Input:     Water level eta = f(tide height, wave amplitude, frequency)
[m]
%           Water current speed U [m/s]
% Output:    Buoy maximum displacement (x, y) [m]
%           Hydrophone package maximum displacement (x, y) [m]

clear
clc

% Environmental parameters
depth = 40;              % [m] nominal depth of site
tide = 0;                % [m] tidal height above equilibrium
waveamp = 1;             % [m] wave amplitude
period = 5;              % [s] wave period
omega = 2*pi/period;     % [rad/s] wave angular velocity
U = 1;                   % [m/s] current speed
g = 9.81;                % [m/s^2] gravitational acceleration
densH2O = 1015;          % [kg/m^3] average density of estuarine water

% Mooring system component masses
m1 = 30;     % [kg] Buoy mass
m2 = 2;      % [kg] Hydrophone 1 mass
m3 = 2;      % [kg] Hydrophone 2 mass
m4 = 2;      % [kg] Hydrophone 3 mass

% Mooring line spring constants
k1 = 50*(9.81/2.2)*(5280/1609);      %
[(lbf/ft)*(9.81N/2.21bf)*(5280ft/1609m)]
k2 = 20000*(9.81/2.2)*(5280/1609);   %
[(lbf/ft)*(9.81N/2.21bf)*(5280ft/1609m)]
k3 = 20000*(9.81/2.2)*(5280/1609);   %
[(lbf/ft)*(9.81N/2.21bf)*(5280ft/1609m)]
k4 = 20000*(9.81/2.2)*(5280/1609);   %
[(lbf/ft)*(9.81N/2.21bf)*(5280ft/1609m)]
k5 = 20000*(9.81/2.2)*(5280/1609);   %
[(lbf/ft)*(9.81N/2.21bf)*(5280ft/1609m)]
k6 = 20000*(9.81/2.2)*(5280/1609);   %
[(lbf/ft)*(9.81N/2.21bf)*(5280ft/1609m)]

% Mooring line damping coefficients
b1 = 10;     % [N-s/m]
b2 = 1;      % [N-s/m]
b3 = 1;      % [N-s/m]
b4 = 1;      % [N-s/m]
b5 = 1;      % [N-s/m]
b6 = 1;      % [N-s/m]
```

```
% Additional mooring line and buoy parameters
L = depth/4;     % [m] nominal spacing of hydrophone packages
rbuoy = 0.425;   % [m] outer buoy radius
Abuoy = 0.5;     % [m^2] cylindrical buoy cross-sectional area
Cd = 0.63;       % [-] buoy drag coefficient

% Define state space arrays from equations of motion
A=zeros(24,24);

 A(1,:) = [0 1 0 0 0 0 0 0 0 0 0 0 0 0 0 0 0 0 0 0 0 0 0 0];
 A(2,:) = [(((-Abuoy*densH2O*g)-k2)/m1)  (-b2/m1) (k2/m1) (b2/m1) 0 0 0
0 0 0 0 0 0 0 0 0 0 0 0 0 0 0 0 0 0 0];
 A(3,:) = [0 0 0 1 0 0 0 0 0 0 0 0 0 0 0 0 0 0 0 0 0 0 0 0];
 A(4,:) = [(k2) (b2) (-k2-k1) (-b1-b2) (k1) (b1) 0 0 0 0 0 0 0 0 0 0 0
0 0 0 0 0 0 0 0];
 A(5,:) = [0 0 0 0 0 1 0 0 0 0 0 0 0 0 0 0 0 0 0 0 0 0 0 0];
 A(6,:) = [0 0 (k1) (b1) (-k1-k3) (-b1-b3) (k3) (b3) 0 0 0 0 0 0 0 0 0
0 0 0 0 0 0 0 0];
 A(7,:) = [0 0 0 0 0 0 0 1 0 0 0 0 0 0 0 0 0 0 0 0 0 0 0 0];
 A(8,:) = [0 0 0 0 (k3/m2) (b3/m2) ((-k3-k4)/m2) ((-b3-b4)/m2) (k4/m2)
(b4/m2) 0 0 0 0 0 0 0 0 0 0 0 0 0 0];
 A(9,:) = [0 0 0 0 0 0 0 0 0 1 0 0 0 0 0 0 0 0 0 0 0 0 0 0];
A(10,:) = [0 0 0 0 0 0 (k4/m3) (b4/m3) ((-k4-k5)/m3) ((-b4-b5)/m3)
(k4/m3) (b4/m3) 0 0 0 0 0 0 0 0 0 0 0 0 0 0];
A(11,:) = [0 0 0 0 0 0 0 0 0 0 0 1 0 0 0 0 0 0 0 0 0 0 0 0];
A(12,:) = [0 0 0 0 0 0 0 0 (k5/m4) (b5/m4) ((-k5-k6)/m4) ((-b5-b6)/m4)
0 0 0 0 0 0 0 0 0 0 0 0];

A(13,:) = [0 0 0 0 0 0 0 0 0 0 0 0 0 1 0 0 0 0 0 0 0 0 0 0];
A(14,:) = [0 0 0 0 0 0 0 0 0 0 0 0 0 (((-0.5*Cd*rbuoy*densH2O*(U^2))-
k2)/m1) (-b2/m1) (k2/m1) (b2/m1) 0 0 0 0 0 0 0 0];
A(15,:) = [0 0 0 0 0 0 0 0 0 0 0 0 0 0 0 0 1 0 0 0 0 0 0 0];
A(16,:) = [0 0 0 0 0 0 0 0 0 0 0 0 0 (k2) (b2) (-k2-k1) (-b1-b2) (k1)
(b1) 0 0 0 0 0 0];
A(17,:) = [0 0 0 0 0 0 0 0 0 0 0 0 0 0 0 0 0 0 1 0 0 0 0 0];
A(18,:) = [0 0 0 0 0 0 0 0 0 0 0 0 0 0 (k1) (b1) (-k1-k3) (-b1-b3) (k3)
(b3) 0 0 0 0];
A(19,:) = [0 0 0 0 0 0 0 0 0 0 0 0 0 0 0 0 0 0 0 0 1 0 0 0 0];
A(20,:) = [0 0 0 0 0 0 0 0 0 0 0 0 0 0 0 0 0 0 (k3/m2) (b3/m2) ((-k3-
k4)/m2) ((-b3-b4)/m2) (k4/m2) (b4/m2) 0 0];
A(21,:) = [0 0 0 0 0 0 0 0 0 0 0 0 0 0 0 0 0 0 0 0 0 1 0 0];
A(22,:) = [0 0 0 0 0 0 0 0 0 0 0 0 0 0 0 0 0 0 0 (k4/m3) (b4/m3) ((-k4-
k5)/m3) ((-b4-b5)/m3) (k4/m3) (b4/m3)];
A(23,:) = [0 0 0 0 0 0 0 0 0 0 0 0 0 0 0 0 0 0 0 0 0 0 0 1];
A(24,:) = [0 0 0 0 0 0 0 0 0 0 0 0 0 0 0 0 0 0 0 0 0 0 (k5/m4) (b5/m4) ((-
k5-k6)/m4) ((-b5-b6)/m4)];

B = zeros(24,1);

 B(1,:) = [0];
 B(2,:) = [(Abuoy*densH2O*g/m1)];
 B(3,:) = [0];
 B(4,:) = [0];
 B(5,:) = [0];
 B(6,:) = [0];
```

```
 B(7,:) = [0];
 B(8,:) = [0];
 B(9,:) = [0];
B(10,:) = [0];
B(11,:) = [0];
B(12,:) = [0];

B(13,:) = [0];
B(14,:) = [(0.5*Cd*rbuoy*densH2O*(U^2)/m1)];
B(15,:) = [0];
B(16,:) = [0];
B(17,:) = [0];
B(18,:) = [0];
B(19,:) = [0];
B(20,:) = [0];
B(21,:) = [0];
B(22,:) = [0];
B(23,:) = [0];
B(24,:) = [0];

C = eye(24,24);

D = zeros(24,1);

% Define state space simulation time parameters
timestep = 0.001
n = 10000
t = 0:timestep:n*timestep;

% Define sea surface height function
eta = tide + waveamp*sin(omega*t);

% Define input to state space simulation
u = [eta];

% Define range of period simulations
Tlow = 0.25;
Tstep = 0.25;
Thigh = 5;

% Define matrices of state values and wave periods
Yset = zeros(n, 24*(Thigh/Tstep));
Tset = zeros(24*(Thigh/Tstep), 1);

% Enter loop to model frequency response
for period=Tlow:Tstep:Thigh

    % Fill vector of wave periods
    for i=1:1:24
        Tset((((period-Tlow)/Tstep)*24)+i), 1) = period;
    end

    % Define sea surface height as function of wave period
```

```
    waveamp = 0.25;
    omega = 2*pi/period;
    eta = tide + waveamp*sin(omega*t);
    u = [eta];

    % State space simulation for given period with .25 [m] wave
amplitude
    Ytemp1 = lsim(A, B, C, D, u, t);

    % State space simulation for given period with .5 [m] wave
amplitude
    waveamp = 0.5;
    eta = tide + waveamp*sin(omega*t);
    u = [eta];
    Ytemp2 = lsim(A, B, C, D, u, t);

    % State space simulation for given period with 1 [m] wave amplitude
    waveamp = 1;
    eta = tide + waveamp*sin(omega*t);
    u = [eta];
    Ytemp3 = lsim(A, B, C, D, u, t);

    % Fill state value matrix
    for i=1:1:n
        for j=(1:1:24)
            Yset1(i, (((period-Tlow)/Tstep)*24)+j) = Ytemp1(i,j);
            Yset2(i, (((period-Tlow)/Tstep)*24)+j) = Ytemp2(i,j);
            Yset3(i, (((period-Tlow)/Tstep)*24)+j) = Ytemp3(i,j);
        end
    end
end

% Calculate max displacement in each state vector
maxset1 = max(Yset1);
maxset2 = max(Yset2);
maxset3 = max(Yset3);

% Declare vectors of frequency response values for maximum
% vertical and horizontal displacements
Tres = zeros((Thigh/Tstep),1);

Ybuoyres1 = zeros((Thigh/Tstep),1);
YH1res1 = zeros((Thigh/Tstep),1);
YH2res1 = zeros((Thigh/Tstep),1);
YH3res1 = zeros((Thigh/Tstep),1);
Xbuoyres1 = zeros((Thigh/Tstep),1);
XH1res1 = zeros((Thigh/Tstep),1);
XH2res1 = zeros((Thigh/Tstep),1);
XH3res1 = zeros((Thigh/Tstep),1);

Ybuoyres2 = zeros((Thigh/Tstep),1);
YH1res2 = zeros((Thigh/Tstep),1);
YH2res2 = zeros((Thigh/Tstep),1);
YH3res2 = zeros((Thigh/Tstep),1);
Xbuoyres2 = zeros((Thigh/Tstep),1);
```

```
XH1res2 = zeros((Thigh/Tstep),1);
XH2res2 = zeros((Thigh/Tstep),1);
XH3res2 = zeros((Thigh/Tstep),1);

Ybuoyres3 = zeros((Thigh/Tstep),1);
YH1res3 = zeros((Thigh/Tstep),1);
YH2res3 = zeros((Thigh/Tstep),1);
YH3res3 = zeros((Thigh/Tstep),1);
Xbuoyres3 = zeros((Thigh/Tstep),1);
XH1res3 = zeros((Thigh/Tstep),1);
XH2res3 = zeros((Thigh/Tstep),1);
XH3res3 = zeros((Thigh/Tstep),1);

% Fill vectors of maximum vertical and horizontal displacements
for period = Tlow:Tstep:Thigh
    Tres(((period-Tlow)/Tstep)+1,1) = Tset((((period-
Tlow)/Tstep)*24)+1);

    % 0.25 [m] wave amplitude vertical and horizontal frequency
response
    Ybuoyres1(((period-Tlow)/Tstep)+1,1) = maxset1((((period-
Tlow)/Tstep)*24)+1);
    YH1res1(((period-Tlow)/Tstep)+1,1) = maxset1((((period-
Tlow)/Tstep)*24)+7);
    YH2res1(((period-Tlow)/Tstep)+1,1) = maxset1((((period-
Tlow)/Tstep)*24)+9);
    YH3res1(((period-Tlow)/Tstep)+1,1) = maxset1((((period-
Tlow)/Tstep)*24)+11);

    Xbuoyres1(((period-Tlow)/Tstep)+1,1) = maxset1((((period-
Tlow)/Tstep)*24)+13);
    XH1res1(((period-Tlow)/Tstep)+1,1) = maxset1((((period-
Tlow)/Tstep)*24)+19);
    XH2res1(((period-Tlow)/Tstep)+1,1) = maxset1((((period-
Tlow)/Tstep)*24)+21);
    XH3res1(((period-Tlow)/Tstep)+1,1) = maxset1((((period-
Tlow)/Tstep)*24)+23);

    % 0.5 [m] wave amplitude vertical and horizontal frequency response
    Ybuoyres2(((period-Tlow)/Tstep)+1,1) = maxset2((((period-
Tlow)/Tstep)*24)+1);
    YH1res2(((period-Tlow)/Tstep)+1,1) = maxset2((((period-
Tlow)/Tstep)*24)+7);
    YH2res2(((period-Tlow)/Tstep)+1,1) = maxset2((((period-
Tlow)/Tstep)*24)+9);
    YH3res2(((period-Tlow)/Tstep)+1,1) = maxset2((((period-
Tlow)/Tstep)*24)+11);

    Xbuoyres2(((period-Tlow)/Tstep)+1,1) = maxset2((((period-
Tlow)/Tstep)*24)+13);
    XH1res2(((period-Tlow)/Tstep)+1,1) = maxset2((((period-
Tlow)/Tstep)*24)+19);
    XH2res2(((period-Tlow)/Tstep)+1,1) = maxset2((((period-
Tlow)/Tstep)*24)+21);
    XH3res2(((period-Tlow)/Tstep)+1,1) = maxset2((((period-
Tlow)/Tstep)*24)+23);
```

```
    % 1 [m] wave amplitude vertical and horizontal frequency response
    Ybuoyres3(((period-Tlow)/Tstep)+1,1) = maxset3((((period-
Tlow)/Tstep)*24)+1);
    YH1res3(((period-Tlow)/Tstep)+1,1) = maxset3((((period-
Tlow)/Tstep)*24)+7);
    YH2res3(((period-Tlow)/Tstep)+1,1) = maxset3((((period-
Tlow)/Tstep)*24)+9);
    YH3res3(((period-Tlow)/Tstep)+1,1) = maxset3((((period-
Tlow)/Tstep)*24)+11);

    Xbuoyres3(((period-Tlow)/Tstep)+1,1) = maxset3((((period-
Tlow)/Tstep)*24)+13);
    XH1res3(((period-Tlow)/Tstep)+1,1) = maxset3((((period-
Tlow)/Tstep)*24)+19);
    XH2res3(((period-Tlow)/Tstep)+1,1) = maxset3((((period-
Tlow)/Tstep)*24)+21);
    XH3res3(((period-Tlow)/Tstep)+1,1) = maxset3((((period-
Tlow)/Tstep)*24)+23);
end

% Plot vertical freq response for buoy over range of wave periods and
% amplitudes
figure
plot(Tres, Ybuoyres1, 'b', Tres, Ybuoyres2, 'r', Tres, Ybuoyres3, 'g')
legend
title('Buoy Vertical Displacement vs. Wave Period for 0.25, 0.5, and 1
[m] Wave Amplitude with Zero Tidal Input and 1 [m/s] Current')
xlabel('Wave Period [s]')
ylabel('Maximum Vertical Displacement [m]');

% Plot vertical freq response for hydrophones over range of wave
periods
figure
plot(Tres, YH1res1, 'r', Tres, YH2res1, 'g', Tres, YH3res1, 'b')
legend
title('Hydrophone Package Vertical Displacement vs. Wave Period for
0.25 [m] Wave Amplitude with Zero Tidal Input and 1 [m/s] Current')
xlabel('Wave Period [s]')
ylabel('Maximum Vertical Displacement [m]');

% Plot vertical freq response for buoy over range of wave periods
figure
plot(Tres, YH1res2, 'r', Tres, YH2res2, 'g', Tres, YH3res2, 'b')
legend
title('Hydrophone Package Vertical Displacement vs. Wave Period for 0.5
[m] Wave Amplitude with Zero Tidal Input and 1 [m/s] Current')
xlabel('Wave Period [s]')
ylabel('Maximum Vertical Displacement [m]');

% Plot vertical freq response for buoy over range of wave periods
figure
plot(Tres, YH1res3, 'r', Tres, YH2res3, 'g', Tres, YH3res3, 'b')
legend
title('Hydrophone Package Vertical Displacement vs. Wave Period for 1
[m] Wave Amplitude with Zero Tidal Input and 1 [m/s] Current')
```

```
xlabel('Wave Period [s]')
ylabel('Maximum Vertical Displacement [m]');

% Plot horizontal freq response for buoy over range of wave periods and
% amplitudes
figure
plot(Tres, Xbuoyres1, 'b', Tres, Xbuoyres2, 'r', Tres, Xbuoyres3, 'g')
legend
title('Buoy Horizontal Displacement vs. Wave Period for 0.25, 0.5, and
1 [m] Wave Amplitude with Zero Tidal Input and 1 [m/s] Current')
xlabel('Wave Period [s]')
ylabel('Maximum Horizontal Displacement [m]');

% Plot horizontal freq response for hydrophones over range of wave
periods
figure
plot(Tres, XH1res1, 'r', Tres, XH2res1, 'g', Tres, XH3res1, 'b')
legend
title('Hydrophone Package Horizontal Displacement vs. Wave Period for
0.25 [m] Wave Amplitude with Zero Tidal Input and 1 [m/s] Current')
xlabel('Wave Period [s]')
ylabel('Maximum Horizontal Displacement [m]');

% Plot horizontal freq response for buoy over range of wave periods
figure
plot(Tres, XH1res2, 'r', Tres, XH2res2, 'g', Tres, XH3res2, 'b')
legend
title('Hydrophone Package Horizontal Displacement vs. Wave Period for
0.5 [m] Wave Amplitude with Zero Tidal Input and 1 [m/s] Current')
xlabel('Wave Period [s]')
ylabel('Maximum Horizontal Displacement [m]');

% Plot horizontal freq response for buoy over range of wave periods
figure
plot(Tres, XH1res3, 'r', Tres, XH2res3, 'g', Tres, XH3res3, 'b')
legend
title('Hydrophone Package Horizontal Displacement vs. Wave Period for 1
[m] Wave Amplitude with Zero Tidal Input')
xlabel('Wave Period [s]')
ylabel('Maximum Horizontal Displacement [m]');
```

Appendix D – Matlab Plots

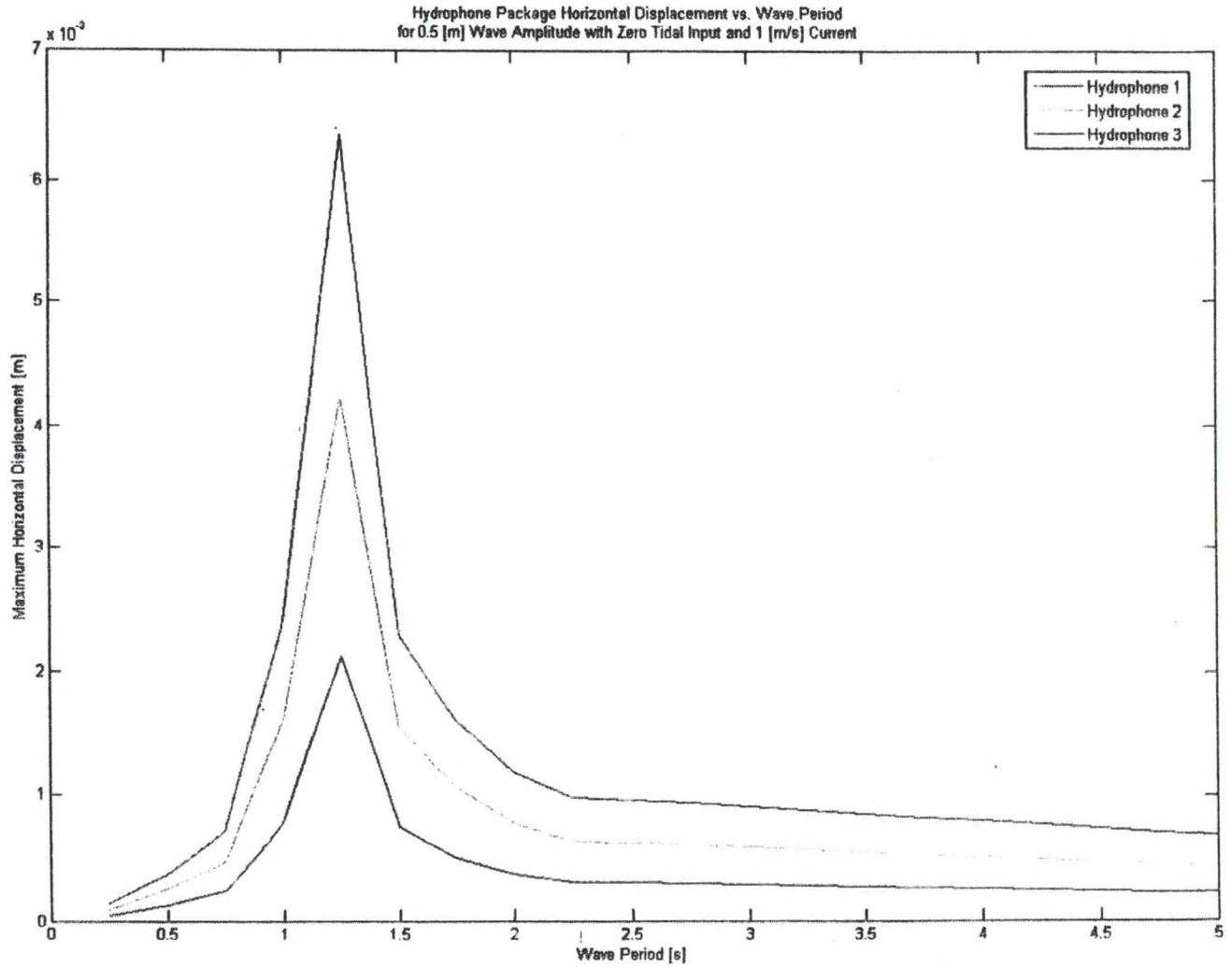

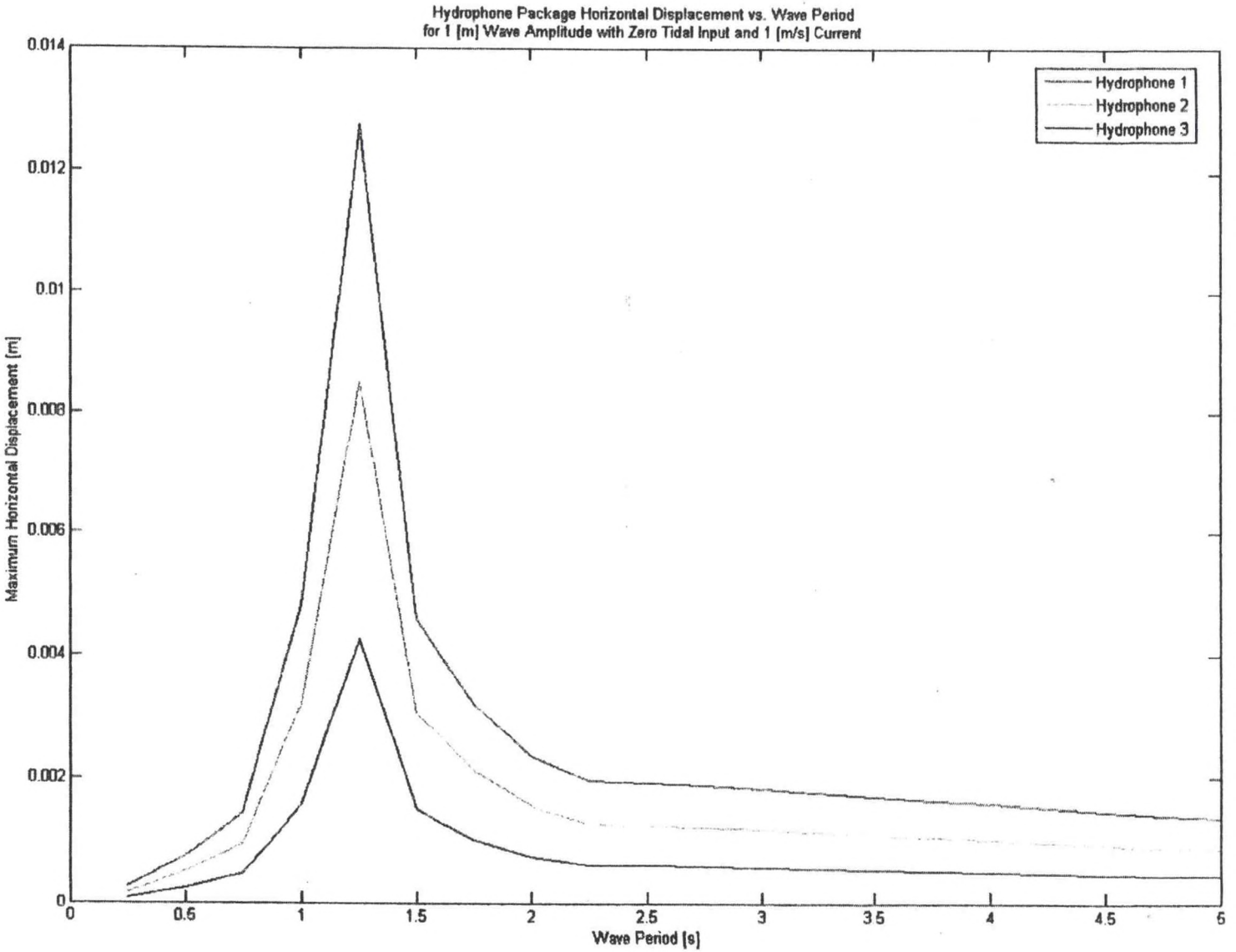
Hydrophone Package Horizontal Displacement vs. Wave Period
for 1 [m] Wave Amplitude with Zero Tidal Input and 1 [m/s] Current
Hydrophone 1
Hydrophone 2
Hydrophone 3
Maximum Horizontal Displacement [m]
Wave Period [s]
0.014
0.012
0.01
0.008
0.006
0.004
0.002
0
0
0.5
1
1.5
2
2.5
3
3.5
4
4.5
5

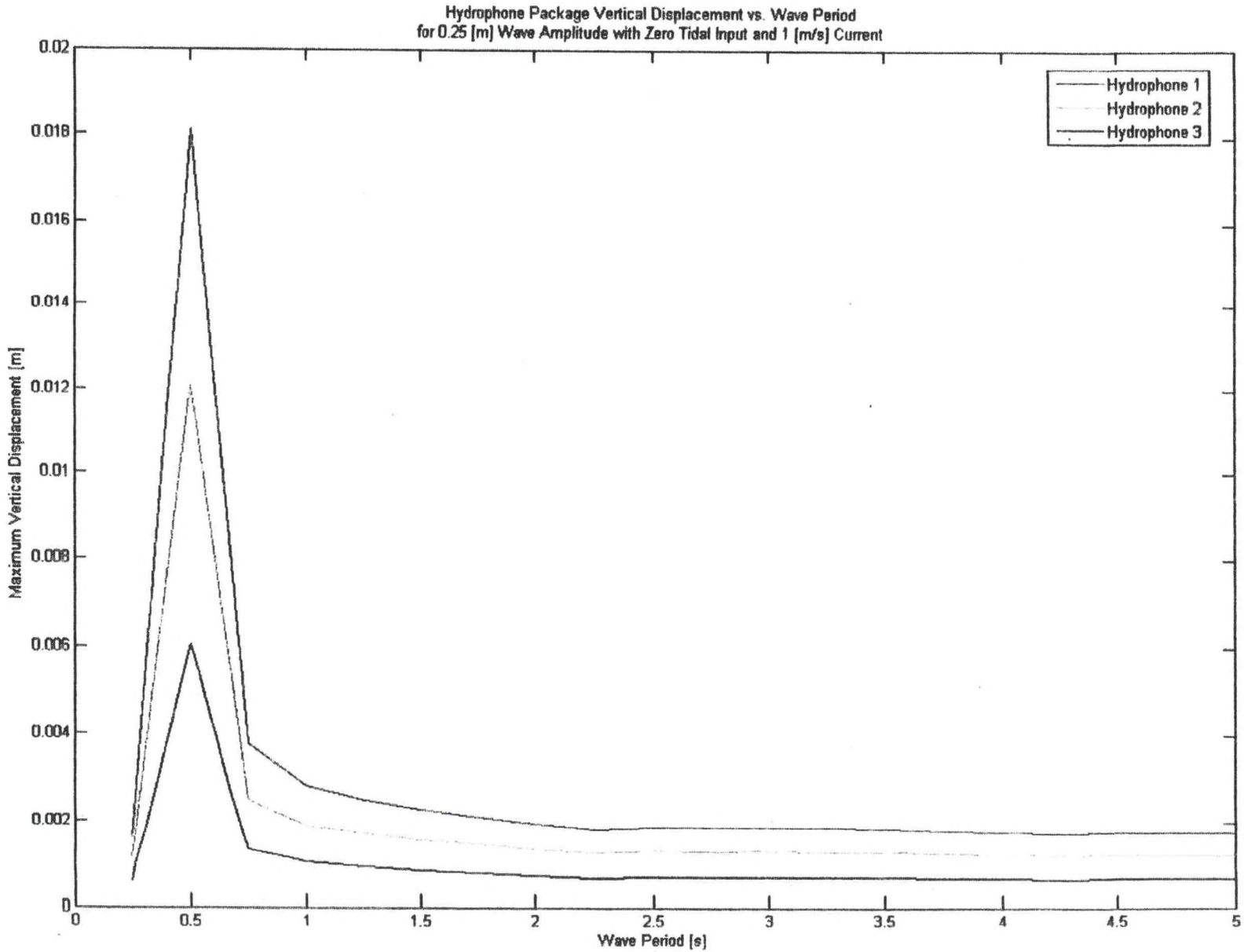
Hydrophone Package Vertical Displacement vs. Wave Period
for 0.25 [m] Wave Amplitude with Zero Tidal Input and 1 [m/s] Current
Maximum Vertical Displacement [m]
Wave Period [s]
Hydrophone 1
Hydrophone 2
Hydrophone 3
0.02
0.018
0.016
0.014
0.012
0.01
0.008
0.006
0.004
0.002
0
0
0.5
1
1.5
2
2.5
3
3.5
4
4.5
5

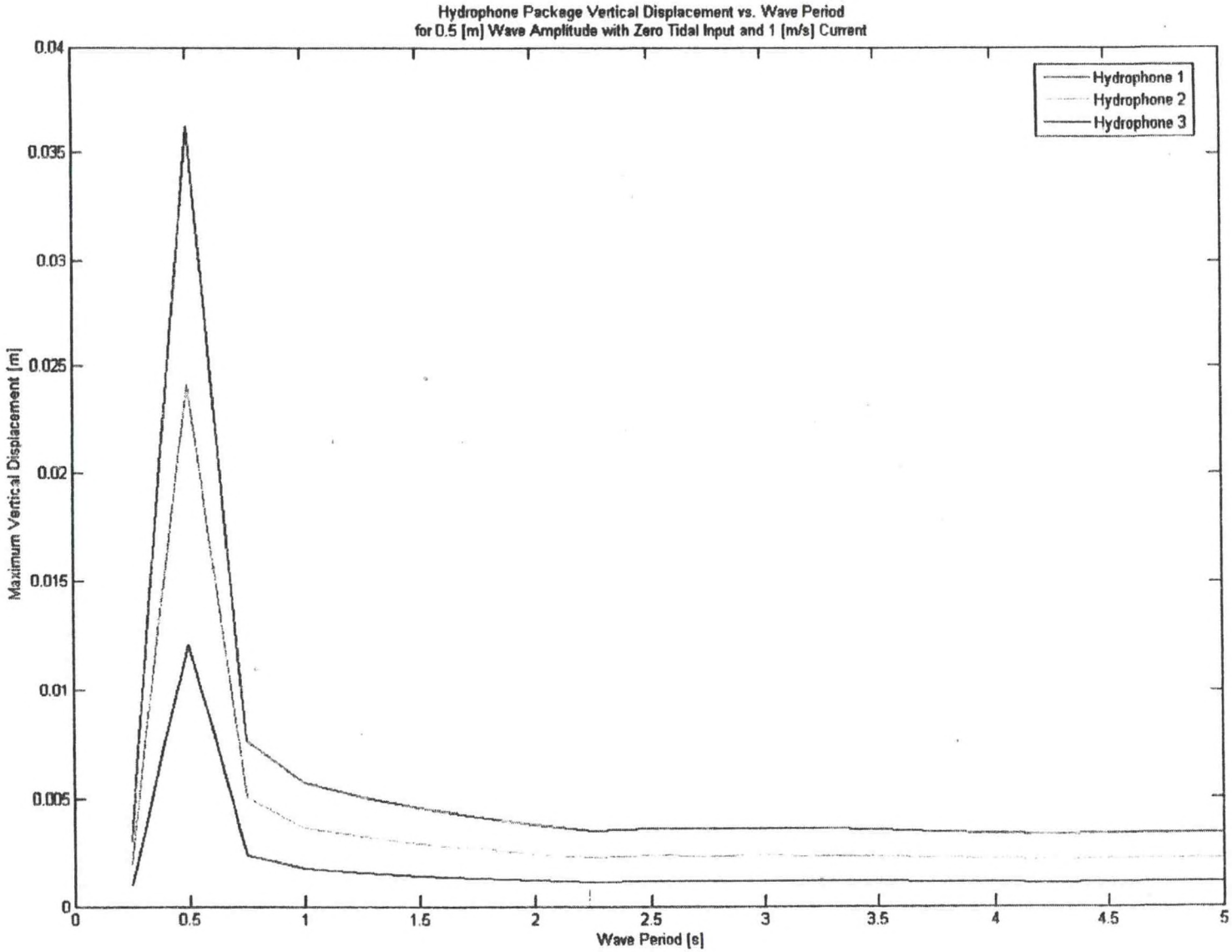
Hydrophone Package Vertical Displacement vs. Wave Period
for 0.5 [m] Wave Amplitude with Zero Tidal Input and 1 [m/s] Current
Hydrophone 1
Hydrophone 2
Hydrophone 3
Maximum Vertical Displacement [m]
Wave Period [s]
0.04
0.035
0.03
0.025
0.02
0.015
0.01
0.005
0
0
0.5
1
1.5
2
2.5
3
3.5
4
4.5
5

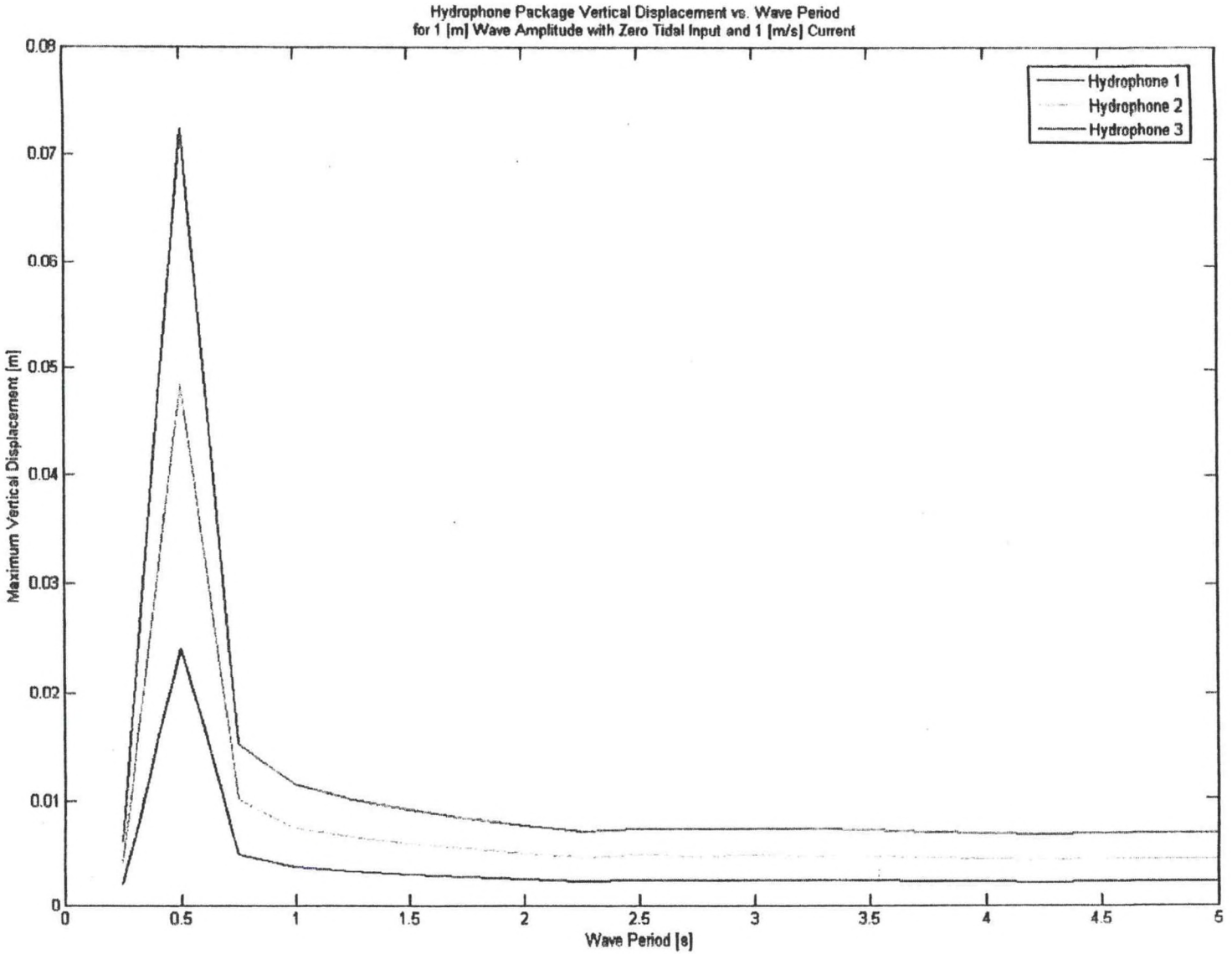
Hydrophone Package Vertical Displacement vs. Wave Period
for 1 [m] Wave Amplitude with Zero Tidal Input and 1 [m/s] Current
Hydrophone 1
Hydrophone 2
Hydrophone 3
Maximum Vertical Displacement [m]
Wave Period [s]
0.09
0.07
0.06
0.05
0.04
0.03
0.02
0.01
0
0
0.5
1
1.5
2
2.5
3
3.5
4
4.5
5

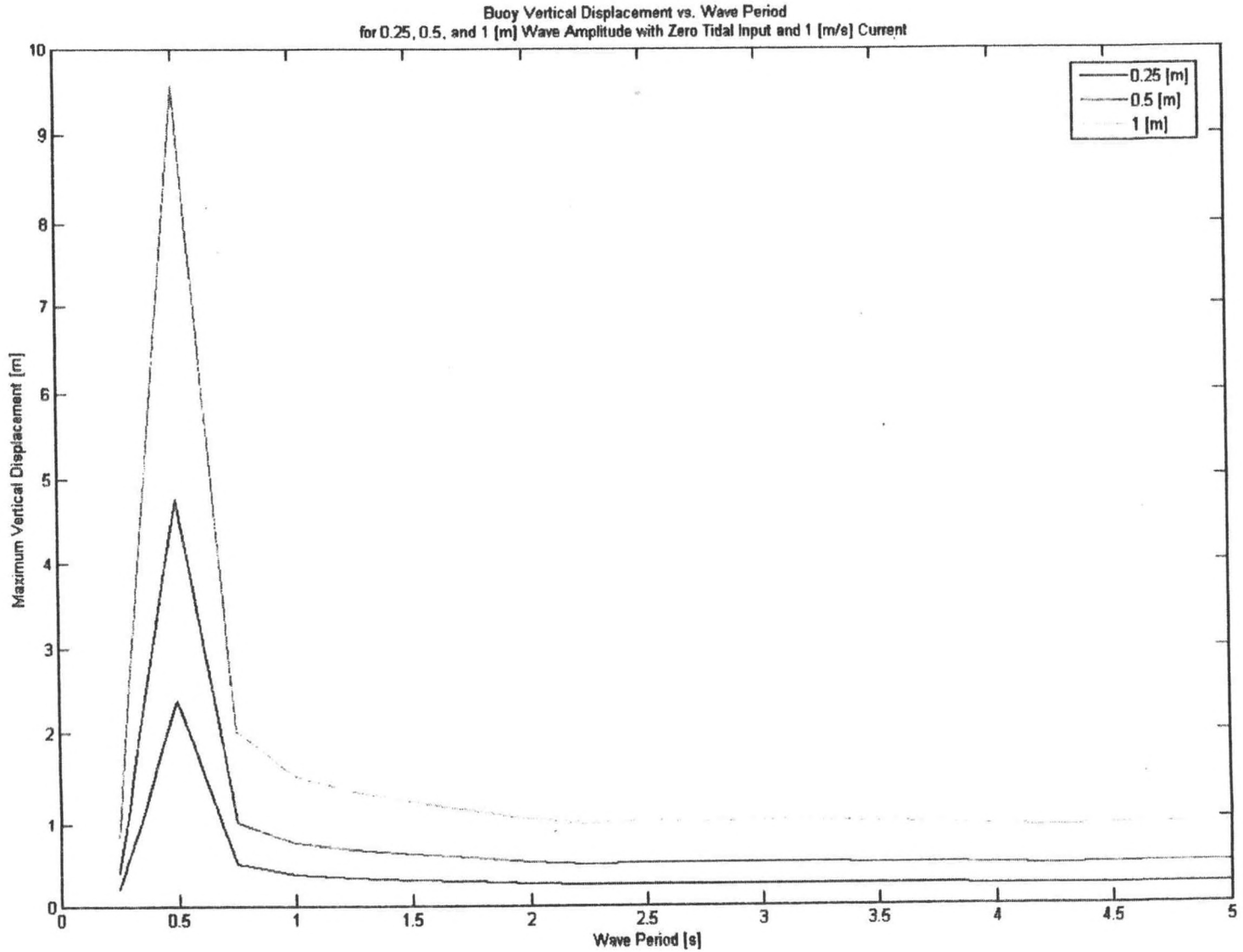
Buoy Vertical Displacement vs. Wave Period
for 0.25, 0.5, and 1 [m] Wave Amplitude with Zero Tidal Input and 1 [m/s] Current
Maximum Vertical Displacement [m]
Wave Period [s]
0.25 [m]
0.5 [m]
1 [m]
0
1
2
3
4
5
6
7
8
9
10
0
0.5
1
1.5
2
2.5
3
3.5
4
4.5
5

Appendix E – Hydrophone Component Specifications

AQ-2000 HYDROPHONE

HYDROPHONES

The AQ-2000 hydrophone represents the latest innovative acoustic sensor technology developed by Benthos for shallow and deep water exploration.

The AQ-2000 is well suited for both towed streamer and ocean bottom cable (OBC) applications that require stable operating performance over a wide range of water depths.

The AQ-2000 has excellent acceleration canceling qualities and exceptionally wide frequency bandwidth.
The AQ-2000 is ready for installation into standard array mounting configurations or integration into custom molded packages.

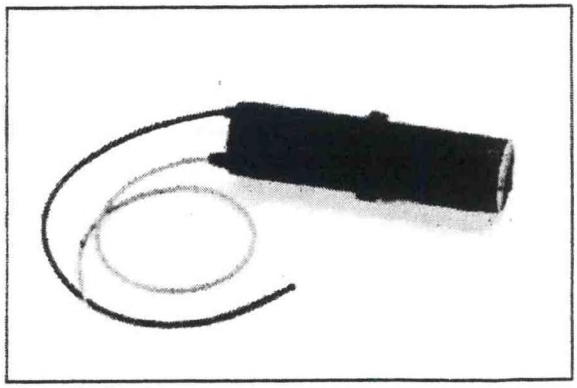

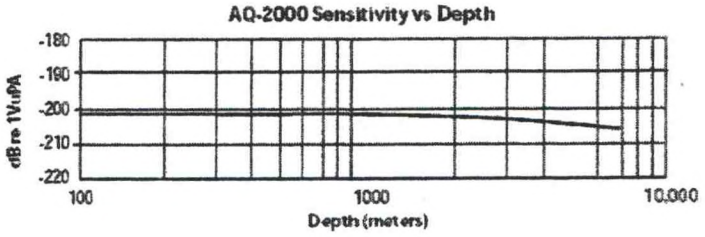

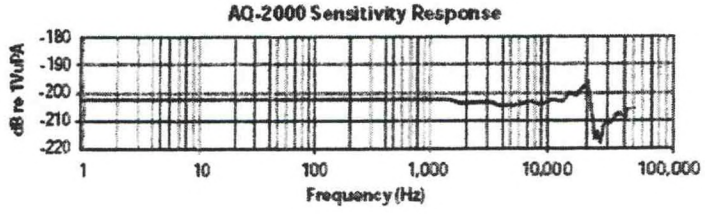

- ACOUSTICS
- FLOTATION
- GEOPHYSICAL
- HYDROPHONES
- IMAGING
- MODEMS
- RELOCATION
- ROBOTICS

BENTHOS

AQ-2000 HYDROPHONE

SPECIFICATIONS

PHYSICAL

Materials:	Flouroelastomer, high strength epoxy, Hytrel® insulated leads
Weight in Air:	14 grams
Size:	4.56 cm long X 1.32 cm diameter
Displacement:	6.24 cc
Temperature:	
Operating:	-10°C to 50°C
Storage:	-40°C to 60°C

ELECTRICAL

Leads:	Two 28 AWG stranded conductors, Hytrel® insulation, red and black, 12.7 cm length
Connector:	None
Polarity:	A positive increase in acoustic pressure generates a positive voltage on the red conductor
Capacitance[2]:	4.5 nF ± 25% at 20°C and 1 kHz
Resistance:	500 Mohm minimum across leads or to sea water at 20°C and 100% relative humidity, 50 VDC
Dissipation:	0.02 typical

PERFORMANCE

Sensitivity @ 100 Hz	
Free-field Voltage[2]:	-201 dB re 1 V/µPa ± 1.5 dB
Sensitivity Change:	
vs. Frequency:	±.25 dB from 1 Hz to 1 kHz (±2.0 dB 1kHz to 10kHz)
vs. Depth:	<.5 dB to 1000 meters
vs. Temperature:	< .03 dB per 1°C change
Acceleration	
Sensitivity:	Output is < 1.5 mV/g due to acceleration in any of the three major axes at 20 Hz
Mechanical	
Resonance:	20 kHz (in water) typical
Max. Operating Depth	2000 m
Destruct Depth:	>7,000 meters

[1] *Every hydrophone is tested for sensitivity, capacitance and insulation resistance at Benthos, Inc. to ensure the highest quality product.*

[2] *Tolerances on electrical parameters are for reference only and tighter tolerances are available upon request to meet specific requirements.*

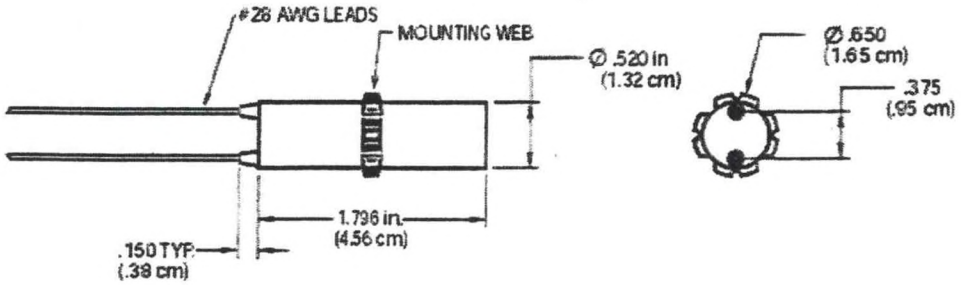

ISO 9001 Certified

Specifications are subject to change without notice.

BENTHOS
Benthos, Inc. • 49 Edgerton Drive, North Falmouth, MA 02556 USA
Tel 508-563-1000 or 800-446-1222 (USA only) • Fax 508-563-6444 • E-mail info@benthos.com
www.benthos.com

Hydrophone Preamplifiers

These Preamplifiers have been specifically designed for small diameter arrays used to extreme depth ratings. High input impedance, low current, and high drive capability make them suitable for long cable lengths.

The AQ-201 and AQ-202 are single ended units with complimentary direct-coupled output drivers. The AQ-202 Model has higher current with lower noise.

The AQ-300 and AQ-302 have the same features as the AQ-201 with the exception of differential input and output circuits.

AQ-201

AQ-300

	AQ-201	AQ-202	AQ-300	AQ-302
Gain dB	26 dB	26 dB	20.8 dB	20.8 dB
Input Impedance	15 MΩ	15 MΩ	30 MΩ	30 MΩ
Current Quiescent mA 12VDC	<0.3 mA	<4.0 mA	<0.6 mA	<8 mA
Noise ref. input nv/√ Hz	<100 nv	<20 nv	<100 nv	<20 nv
High Pass -3 dB	1 Hz	1 Hz	.3 Hz	.3 Hz
Low Pass -3 dB	12 kHz	12 kHz	14 kHz	14 kHz
Depth in meters	1732	1732	1732	1732
Size in cm O.D./length	1.74/4.46	1.74/4.45	1.66/5.7	1.65/5.7
Weight in grams	17.4	17.4	17.1	17.1

Processor	• VIA C3™/ VIA Eden™ EBGA processor
Chipset	• VIA CLE266 North Bridge • VIA VT8235 South Bridge
System Memory	• 1 DDR266 DIMM socket • Up to 1GB memory size
VGA	• Integrated VIA Unichrome AGP graphics w/MPEG-2 Accelerator
Expansion Slots	• 1 PCI
Onboard IDE	• 2 X UltraDMA 133/100/66 Connector
Onboard Floppy	• 1 x FDD Connector
Onboard LAN	• VIA VT6103 10/100 Base-T Ethernet PHY
Onboard Audio	• VIA VT1616 6 channel AC'97 Codec
Onboard TV Out	• VIA VT1622A TV Out
Onboard IEEE 1394	• VIA VT6307S IEEE 1394 (Optional)
Onboard CardBus / CompactFlash	• CardBus Type I & Type II • Ricoh R5C476 II / R5C485 CardBus Corntroller
Back Panel I/O	• 1 CardBus Type I and Type II slot +1 CompactFlash Slot • 1 CompactFlash slot • 1 RJ-45 LAN port

	• 1 PS2 mouse port • 1 PS2 keyboard port • 1 Serial port • 2 USB 2.0 ports • 1 VGA port • 1 RCA port (SPDIF or TV-Out) • 1 S-Video port • 1 1394 port • 3 Audio jacks: line-out, line-in and mic-in (Smart 5.1 Support)
Onboard I/O Connectors	• 1 USB connector for 2 additional USB 2.0 ports • 1 Front-panel audio connectors (mic-in and line-out) • 1 CD Audio-in connector • 1 Buzzer • 1 FIR connector • 1 CIR connector (Switchable for KB/MS) • 1 Wake-on-LAN connector • 1 LPT port header • CPU/Sys FAN/Fan 3 • 1 Connector for LVDS module (Optional) • 1 Serial port connector for second COM port • ATX Power Connector
BIOS	• Award BIOS • 2/4Mbit flash memory
System Monitoring & Management	• CPU voltage monitoring • Wake-on-LAN, Keyboard Power-on, Timer Power-on • System power management • AC power failure recovery
Operating Temperature	• 0~50°C
Operating Humidity	• 0% ~ 93% (relative humidity; non-condensing)
Form Factor	• Mini-ITX (6 layer) • 17 cm x 17 cm

Portable USB-Based DAQ with Simultaneous Sampling

NI USB-9215A, NI USB-9215 *NEW!*

- Small, portable devices (12.1 by 8.6 by 2.5 cm)
- 4 channels of 16-bit simultaneously sampled analog input
- Built-in, removable connectors for easier and more cost-effective connectivity
- 250 V_{rms} channel-to-earth ground isolation
- Plug-and-play connectivity via USB
- Bus-powered

Operating Systems
- Windows 2000/XP
- Mac OS X
- Linux

Recommended Software
- LabVIEW
- LabWindows/CVI
- Measurement Studio

Measurement Services Software (included)[1]
- NI-DAQmx driver software
- VI Logger Lite data-logging software

[1] *Mac OS X and Linux users must download NI-DAQmx Base driver.*

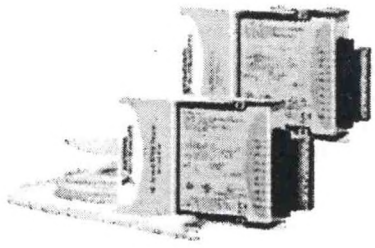

Product	Signal Type	Channels (DI)	Input Resolution (bits)	Sampling Rate (kS/s/ch)	Input Range (V)	Connector	Operating System	Driver Software[1]
USB-9215A	Voltage	4	16	100	±10	Screw terminal, BNC	Windows	NI-DAQmx
USB-9215	Voltage	4	16	25 (typ)	±10	Screw terminal	Mac OS X and Linux	NI-DAQmx Base

[1] Go to ni.com/info and enter the Info Code rdsoftver for up-to-date information on NI-DAQ, visit ni.com/support/daq/versionhistory.htm

Table 1. Portable USB DAQ for Simultaneous Sampling Selection Guide

Hardware Description

National Instruments USB-9215A and USB-9215 are data acquisition modules with integrated signal conditioning that provide plug-and-play connectivity via USB for faster setup and measurements. They offer four channels of simultaneously sampled voltage inputs with 16-bit accuracy to provide minimal phase delay when scanning multiple channels. In addition, these modules include 250 V_{rms} channel-to-earth ground isolation for safety, noise immunity and high common-mode voltage range.

Software Description

The NI USB-9215A uses NI-DAQmx high-performance, multithreaded driver software for interactive configuration and data acquisition on Windows OSs. All NI data acquisition devices shipped with NI-DAQmx also include VI Logger Lite configuration-based data-logging software. The NI USB-9215 for Mac OS X and Linux uses NI-DAQmx Base, a multiplatform driver with a limited NI-DAQmx programming interface. You can use NI-DAQmx Base to develop customized data acquisition applications with National Instruments LabVIEW or C-based development environments. NI-DAQmx Base includes a ready-to-run data logger application that acquires and logs up to four channels of analog data.

Recommended Accessories

The USB-9215A and USB-9215 both have built-in screw-terminal connectivity, so no additional accessories are required. The USB-9215A is also available with BNC connectors.

Common Applications

The USB-9215A and USB-9215 are ideal for a number of applications where small size and portability are essential, such as:
- Portable data logging – log voltage data quickly and easily
- Academic lab use – obtain academic discounts for quantities of five or more. Visit ni.com/academic for details.
- Environmental monitoring – monitor environmental conditions such as humidity or light
- Embedded OEM applications
- In-vehicle data acquisition

Information for OEM Customers

For information on special configurations and pricing, please visit ni.com/oem.

Ordering Information

NI USB-9215A[1]
- Screw Terminals 779434-01
- BNC Connectors 779435-01

NI USB-9215[2]
- Screw Terminals 778977-01

[1] *Windows only*
[2] *Mac OS X and Linux only*

BUY NOW!

For complete product specifications, pricing, and accessory information, call (800) 813 3693 (U.S. only) or go to ni.com/info.

NATIONAL INSTRUMENTS

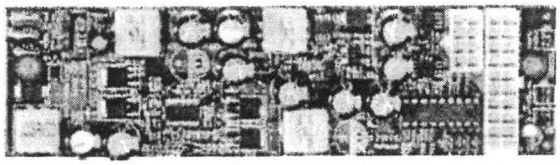

Works with all VIA mini-ITX boards and CPUs

MI-ATX
Intelligent 90 Watts Automotive ATX Power Supply

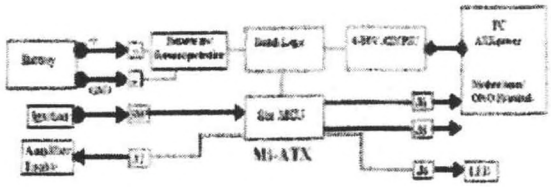

Intelligent Automotive Power Supply

Designed to provide power and to control the ON/OFF switch of a motherboard (based on ignition status), MI-ATX is a 6-24V input ATX PSU capable of surviving tough engine cranks (down to 5.7V) as well as transient over-voltage situations.

Multiple Shutdown Schemes

MI-ATX has 8 user selectable microcontroller driven timing modes, allowing you to choose up to 8 ignition/shutdown timing schemes. By removing all user-selectable jumpers, MI-ATX becomes a traditional PSU with no ignition control and it can be used in non-car applications.

Even if your computer is totally OFF, a PC will still consume few hundered milliwatts, needed to monitor PC ON/OFF status. When the computer is in the suspend/sleep mode, it will consume even more power, because the RAM needs to be powered at all times. The power consumption in the suspend mode is few watts. No matter how big your battery is, it will eventually drain your battery in a matter of days.

Deep Sleep Mode

While in deep sleep mode, MI-ATX constantly monitors your car battery voltage levels, preventing deep discharge situations by automatically shutting down until battery levels reach safe levels again.

No more dead batteries, no more computer resets during engine cranks, along with multiple timing schemes, small formfactor and competitive price makes the MI-ATX the premier solution for ATX vehicle power supply solutions.

Minimum input Operating voltage	5.7V
Maximum input Operating voltage	30V
Min startup voltage	6V
Deep-Discharge shutdown threshold	11V
Input current limit (fuse protected)	10A
Max Output Power	90 Watts
Operating temperature	-20 to +85 degrees Celsius
Storage temperature	-40 to +125 degrees Celsius
MTBF	192,000 hrs @ 55C, 96,000 hrs @ 85C
Efficiency (input 7-24V)	>80% on 3.3,5,5VSB ~80% on 12V
PCB size	160x48mm
Input connectors	Faston 0.25" terminal
Input fuse	Mini-Blade fuse, 10A
Output Connector	ATX Power 20 pin (Molex P/N 39-01-2200)
J1, J4, J2, J3	Polarized Header 2x1, 0.1"

Mechanical Characteristics

-Board measurements: 1.77"x6.31"
-Height: < 1", 1U formfactor compatible
-Formfactor compatible with mini-ITX Casetronics enclosures
-Designed for the mini-box VehiclePC extruded enclosure

CPU and Board Support

-VIA X86 CPUs, PII, PIII and low power P4/AMD*
-Supports all VIA mini-ITX motherboards
*NOTE: Check the total 12V rail power consumption

Wire harness

MI-ATX comes equipped with ATX, HDD and Floppy cable harness, jumpers, faston connectors and 2 pin cables for motherboard ON/OFF switch. Just connect it to your car / boat / RV battery and power up your PC.

OEM Integration

Other timing schemes / designs are possible.
OEM integration is welcome. Please send an email to mi-atx@mini-box.com with your custom requirements.

Maximum Power Characteristics

Output Rail	Current (Max)	Current Peak (400 seconds)	Ripple (V p-p)	Regulation
5V	10A	15A	50mV	1.5%
3.3V	10A	15A	50mV	1.5%
5VSB	1.5A	2A	50mV	1.5%
-12V	0.15A	0.2A	120mV	10%
12V	6A	7.5A	100mV	1.5%

Corporate address: 43230 Christy St, Fremont, CA 94538
http://www.mini-box.com, email: sales@mini-box.com

Travelstar 5K100 hard disk drives specifications

Travelstar 5K100 models	Capacity (GB)	RPM	Interface
HTS541010G9AT00	100	5400	Parallel-ATA
HTS541080G9AT00	80	5400	Parallel-ATA
HTS541060G9AT00	60	5400	Parallel-ATA
HTS541040G9AT00	40	5400	Parallel-ATA
HTS541010G9SA00	100	5400	Serial-ATA
HTS541080G9SA00	80	5400	Serial-ATA
HTS541060G9SA00	60	5400	Serial-ATA
HTS541040G9SA00	40	5400	Serial-ATA

Configuration	Parallel-ATA	Serial-ATA
Interface	ATA-6	Serial ATA 1.5Gb/s
Capacity (GB)[1]	100 / 80 / 60 / 40	←
Sector size (Bytes)	512	←
Recording zones	16	←
Data heads (physical)	4 / 4 / 3 / 2	←
Data disks	2 / 2 / 2 / 1	←
Max. areal density (Gbits/sq. inch)	86 / 70 / 70 / 70	←
Performance		
Data buffer (MB)[2]	8	←
Rotational speed (RPM)	5400	←
Latency average (ms)	5.5	←
Media transfer rate (Mbits/sec, max)	493	←
Interface transfer rate (MB/sec, max)	100 Ultra DMA mode-5 16.6 PIO mode-4	150
Seek time (typical)		
Average (ms)	12	←
Reliability		
Load/Unload cycle	600,000	←
Power		
Requirement	+5VDC (+-5%)	←
Dissipation (Typical)		
Startup (peak, max.)	5.0W	←
Read (avg.)	2.0W	←
Write (avg.)	2.0W	←
Active idle (avg.)	0.85W	1.2W
Low power idle (avg.)	0.60W	0.85W
Standby (avg.)	0.2W	0.4W
Sleep	0.1W	0.2W
Physical size		
Height (mm)	9.5	←
Width (mm)	70	←

Depth (mm)	100	←
Weight - typical (g)	102 / 102 / 102 / 95	

Environmental characteristics

Operating		
Ambient temperature	5° to 55° C	←
Shock (half sine wave)	300 G / 2ms, 160G / 1ms	←
Non-operating		
Ambient temperature	-40° to 65° C	←
Shock (half sine wave)	1000 G / 1 ms	←
Acoustics (A-Weighted Sound Power (Bels))		
Idle (typ.)	2.5 / 2.5 / 2.5 / 2.2	
Op (typ.)	2.7 / 2.7 / 2.7 / 2.4	←
RoHS compliant[3]	yes	

[1]

[3] RoHS refers to the European Union Directive 2002/95/EC on the restriction of certain hazardous substances in electrical and electronic equipment.